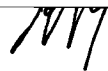AN ABSTRACT OF THE DISSERTATION OF

Julian E. Stelzer for the degree of Doctor of Philosophy in Human Performance
presented on May 20, 2002.
Title: Protein Isoform-Function Relationships of Single Skeletal Muscle Fibers
from Weight-Bearing and Hindlimb Suspended Mice

Redacted for Privacy

Abstract approved _____
/V̄ / Jeffrey J. Widrick

The **goals** of this research were to a) characterize the protein-function

relationships of skeletal muscle single fibers from the mouse hindlimb b) examine

mouse-strain related differences in myosin heavy chain composition (MHC) and

single fiber contractile function, and c) quantify changes in fiber size and

contractile function in response to 7 days of non-weight bearing. This research is

significant because mechanistic approaches to understanding relationships between

muscle protein expression, contractile function, and mechanical loading will likely

benefit from a transition from the traditional laboratory rat to genetically modified

mouse models.

The **methods** used in this research feature an in vitro skinned-fiber

preparation and single-fiber gel electrophoresis. Hindlimb muscles of mice were

excised, and dissected into smaller bundles from which single muscle fibers were

isolated. Single fibers were placed in skinning solution that permeabilized the

fiber's membrane. The ends of skinned single muscle segments were attached to

stainless steel troughs, which were connected to an isometric force transducer and a direct-current position motor. This system allowed the measurement of the fiber's cross-sectional area (CSA), peak isometric force (P_o), and unloaded maximal shortening velocity (V_o) during maximal Ca^{2+}-activating. The identification of the fiber's MHC content was subsequently achieved by electrophoresis of a sample of each fiber segment.

The **results** showed that the C57BL/6 mouse soleus muscle contains a MHC composition (20% type I) that is dramatically different than the ICR and CBA/J mouse strains (50% type I, respectively). Type I fibers from the C57BL/6 mouse had V_o that was 25% lower than type I fibers from ICR and CBA/J mice. Following 7 days of hindlimb suspension (HS) all strains experienced significant soleus muscle and single-fiber atrophy and decreases in the absolute and specific (force/fiber CSA) of type I and II fibers. However, type I fibers from C57BL/6 mice showed no change in V_o whereas type I fibers from ICR and CBA/J showed increased V_o.

In **conclusion**, this research demonstrates that unlike the rat and human models of non-weight bearing, mouse soleus type I and II fibers are equally affected by HS with respect to decreases in fiber CSA and force. However, type I fiber V_o was elevated only in mouse strains with solei containing at least 50% type I MHC. These findings challenge the current view that non-weight bearing affects slow fibers more than fast fibers, and suggests that changes in single fiber

contractile function with HS may be influenced in part by the MHC distribution of

the muscle.

Protein Isoform-Function Relationships of Single Skeletal Muscle Fibers from
Weight-Bearing and Hindlimb Suspended Mice

By

Julian E. Stelzer

A DISSERTATION

Submitted to

Oregon State University

in partial fulfillment of
the requirements for the
degree of

Doctor of Philosophy

Presented May 20, 2002
Commencement June 2003

Doctor of Philosophy dissertation of Julian E. Stelzer presented on May 20, 2002.

APPROVED:

Redacted for Privacy

Major Professor, representing Human Performance

Redacted for Privacy

Chair of the Department of Exercise and Sport Science

Redacted for Privacy

Dean of the Graduate school

I understand that my dissertation will become part of the permanent collection of Oregon State University libraries. My signature below authorizes release of my dissertation to any reader upon request.

Redacted for Privacy

Julian E. Stelzer, Author

CONTRIBUTIONS OF AUTHORS

Dr. Jeffrey Widrick was involved in the hindlimb suspension of the animals, performed the surgical procedures and preparations of muscle homogenates for electrophoretic analysis, and assisted in the writing of the manuscripts.

TABLE OF CONTENTS

TABLE OF CONTENTS (*Continued*)

LIST OF FIGURES

LIST OF TABLES

Protein Isoform-Function Relationships of Single Skeletal Muscle Fibers
from Weight-Bearing and Hindlimb Suspended Mice

Chapter 1

Introduction

Julian E. Stelzer

Department of Exercise and Sport Science

Hindlimb suspension

Rodent hindlimb suspension (HS) is a popular model to study non-weight bearing especially as it affects muscle function. The hindlimb suspension model was developed in the in the late 1970's as a ground-based model to study the effects of space flight on muscle and bone function (Musacchia et al., 1980; Morey, 1979). Currently the model is also used to mimic the effects of chronic inactivity, such as prolonged bedrest.

In the HS model, the animal is suspended by a tail or body harness such that the forelimbs touch the ground, so the animal can maneuver around the cage but so the hindlimbs do not bear any weight. Although the hindlimbs cannot contract against external resistance, they are still free to move and stretch while suspended. The HS model effectively mimics space flight as there is total unloading of the rear limbs without restriction of movement, coupled with a cephalic redistribution of body fluids. The animal is also able to eat, drink, and groom in a normal fashion, and is not under significant physiological and psychological stress (Morey, 1979).

It is well established that muscle atrophy occurs as a consequence of hypokinesia (decreased movement) and decreased physical load (weight-bearing). Thus, HS is one of the primary models in the study of the mechanisms that govern muscle atrophy.

Non-weight bearing and muscle atrophy

Non-weight bearing produces significant atrophy of mammalian hindlimb muscles with most of the muscle mass loss occurring in the first week of unloading (Thomason and Booth, 1990). The mechanisms responsible for muscle atrophy during non-weight bearing are not completely understood. The absence of loaded contractions and decreased electrical activity in the muscle are likely involved (Riley et al., 1990). However, atrophy occurs even when loaded contractions are used as countermeasures (Widrick et al., 1996) suggesting that other mechanisms are also involved.

<u>Muscle atrophy mechanisms</u>

It appears that the magnitude of the muscle mass loss response depends on the fiber type of the muscle, with extensor muscles comprised mostly of slow fibers, such as the soleus, vastus intermedius, and abductor longus, showing the most atrophy. Conversely, flexor muscles with fast fiber type composition such as the tibialis anterior and extensor digitorum longus show the least atrophy (Fitts et al., 2000). It appears that the function of the muscle is related to the response to non-weight bearing because muscles that play an antigravity, postural role in normal loading conditions tend to atrophy the most.

The mechanisms responsible for muscle atrophy during non-weight bearing are not completely understood. Muscle atrophy is primarily a result of decreases in

cross sectional area and not changes in fiber length or number (Templeton et al., 1988). In the rat model, initial protein loss in the first few days of unloading is attributed to decreased protein synthesis, however, after the third day of suspension it appears that protein synthesis establishes a new steady state, and protein degradation increases sharply to become the important contributor to muscle atrophy (Thomason et al., 1989). After 14 days, protein degradation decreases so that a new steady state is attained and atrophy slows. Thus, in rats it appears that the rate of peak muscle atrophy occurs at about the 14th day of hindlimb suspension (Thomason et al., 1989).

HS causes selective loss of contractile protein in rats and mice (McCarthy et al., 1997). Decreases in protein synthesis appear to be a result of a decreased translation rate of mRNA through a slowing of the nascent polypeptide chain elongation rate (Ku and Thomason, 1994). McCarthy et al. (1997) found a decrease in soleus β-MHC mRNA message in mice after 14 days of HS. A 600 base pair region of the promoter sequence was responsible for the decreased transcription of β-MHC transgenes in response to unloading. Thus, it appears that a negative regulatory response element exists that mediates decreased β-MHC expression in response to unloading. Other evidence suggests that myosin and actin protein synthesis is regulated by separate mechanisms. For example, it has been shown that 7 days of hindlimb suspension did not alter β-myosin MHC mRNA but significantly decreased α-actin mRNA (Thomason et al., 1989). Furthermore, Riley

et al. (2000) showed that after 17 days of space flight there was a selective loss of actin filaments in human soleus muscle fibers.

Whole muscle atrophy

Most HS studies have been done on rats. These studies generally show that the rat soleus muscle, which is composed of 85-90% slow type I fibers (Delp and Duan, 1996), experiences more atrophy than other hindlimb muscles, such as the gastrocnemius and plantaris which contain a majority of fast type II fibers (Delp and Duan, 1996). Following 7-14 days of HS the rat soleus muscle atrophies 26-44% (Thompson et al., 1998; McDonald et al., 1994; Widrick et al., 1996) and soleus to body mass ratio decreases 12-52% (Thompson et al., 1998; McDonald et al., 1994; Widrick et al., 1996; Fitts et al., 1986). The rat gastrocnemius atrophies 14-26% (Steffen et al., 1986; Thompson et al., 1998) while the plantaris atrophies 19% (Thompson et al., 1998) following 7-14 days of HS.

Single fiber atrophy

On the single fiber level it appears that rat type I fibers are more susceptible to atrophy with unloading than type II fibers. Type I fibers atrophy 16-60% (McDonald and Fitts, 1995; Widrick et al., 1996; Desplanches et al., 1987) and type II fibers atrophy 17-34% (Gardetto et al., 1989; Desplanches et al., 1987) following 7-14 days of HS. Edgerton and Roy (1996) observed that the diameter of the fiber prior to non-weight bearing plays a role in determining the amount of

atrophy occurring with non-weight bearing as fibers with larger diameters are more affected than smaller fibers. In rats type I fibers experience more atrophy following non-weight bearing than the smaller type II fibers, while in humans type II fibers experience more atrophy following non-weight bearing than the smaller type I fibers. Since both the rat and human soleus muscles contain such a small amount of type II fibers, researchers are often forced to study fast fibers from other hindlimb muscles such as the plantaris or gastrocnemius. However, this can complicate interpretations because it is known that these other hindlimb muscles are not as affected by non-weight bearing as the soleus muscle. Thus, it is difficult to determine if rat type I fibers are intrinsically more susceptible to atrophy with non-weight bearing or whether their rate of atrophy is dependent upon the role played by the muscle in which they reside.

Non-weight bearing and whole muscle contractile function

After HS the slow soleus shows faster mechanical properties, while properties of muscles that are composed of predominantly fast fibers are largely unaffected (Thomason and Booth, 1990). Peak isometric twitch duration is a reflection of the intracellular calcium transient, and depends on the rate and amount of calcium release from the sarcoplasmic reticulum (SR), the rate it binds and is released from troponin, and rate of calcium reuptake by the SR. The functional components of the twitch duration are time to peak tension, and relaxation time.

Caiozzo et al. (1994) found that after 6 days of space flight, twitch tension decreased 19%, half relaxation time decreased 10%, and time-to-peak tension decreased 9% in rat soleus muscle. Caiozzo et al. (1996) then examined the same parameters after 14 days of space flight and found that peak twitch tension decreased 33%, half relaxation time decreased 30%, and time to peak tension decreased 19% in rat soleus muscle. Consistent with shortened twitch durations, Schulte et al. (1993) found that 28 days of HS shifted the force-frequency curve to the right in rat soleus muscle. Caiozzo et al. (1994, 1996) also found that 6 and 14 days of space flight shifted the force-frequency curve to the right in rat soleus muscle. A right shift in the force-frequency curve suggests that non-weight bearing increases the rate of calcium uptake in the SR. Schulte et al. (1993) reported that after 28 days of HS there was a 300% increase in fast SR calcium pump protein, and a 170% increase in calcium dependent SR ATPase activity. Furthermore, Kandarian et al. (1992) found that after 28 days of HS, T-tubular dihydropyridine (DHP)-receptor mRNA in the soleus muscle matched that from the fast extensor digitorum longus muscle. These changes taken together are likely to explain why soleus time-to-peak tension and half relaxation time both decrease with HS (Schulte et al., 1993). The decrease in twitch force could be due to changes in regulatory proteins, and direct effects at the cross-bridge which slow the transition from a low-to high-force state (Fitts, 1994).

During a single twitch, which is triggered by a single action potential, the active state of the muscle is rapidly terminated by the calcium-sequestering activity

of the SR, which removes calcium from the myoplasm soon after it is released. Thus, the active state of the muscle actually begins to decline before the filaments have had time to slide past each other and produce tension. If a second action potential follows the first, but before the SR can entirely remove previously released calcium from the myoplasm, then the concentration of calcium remains elevated in the myoplasm prolonging the active state and producing more tension. The muscle is said to reach full tetanus tension when increasing the frequency of action potential no longer increases tension, and the single twitches essentially fuse with one another. This condition is defined as peak tetanic tension.

Peak tetanic tension has been reported to decrease in the rat soleus following non-weight bearing. Caiozzo et al. (1994, 1996) found that 6 and 14 days of space flight decreased peak tetanic tension by 28% and 36%, respectively, in rat soleus muscle. Fitts et al. (1986) reported that after 14 days of HS peak tetanic isometric tension decreased by 49% in the soleus with no significant changes in the fast extensor digitorum longus muscle. The maximum tetanic tension of the soleus is decreased to a larger extent than would be expected by decreases in mass following unloading. Thus specific tension, or tension per unit of cross sectional area, is decreased (Thomason and Booth, 1990). This effect is not seen in predominantly fast muscles like the extensor digitorum longus and the gastrocnemius.

After non-weight bearing the soleus muscle generally shows an overall increased maximal velocity of contraction. Maximal shortening velocity of the rat

soleus was found to be increased 13% and 124% after 1 and 2 weeks of HS, while there was no change in fast extensor digitorum longus shortening velocity at either time point (Fitts et al., 1986). Caiozzo et al. (1994, 1996) found that maximal velocity of rat soleus muscle increased 14% and 20% after 6 and 14 days of space flight, respectively. Thomason et al. (1986) showed that muscles having the largest proportion of fast myosin heavy chains also had the highest maximal contraction velocities partly because of higher ATPase activities.

The latter observation agrees with the reported overall decrease in the expression of type I fibers and an increase in the expression type IIa and type IIx in the rat soleus (Caiozzo et al., 1998; Talmadge et al., 1996). Templeton et al. (1984) reported that after 3 weeks of non-weight bearing, type I myosin decreased from 88% to 62% in rat soleus. Caiozzo et al. (1994) observed a 10% increase in type IIx myosin and a decrease in type I and IIa myosin after 6 days of space flight. Caiozzo et al. (1996) found that after 14 days of space flight, type I myosin decreased 4%, and type IIx myosin increased 4% in rat soleus. Talmadge et al. (1996) reported that after 2 weeks of HS type IIx myosin increased 5%, type I myosin decreased 5%, and type IIa myosin remained unchanged in rat soleus. Aside from increases in type IIa and IIx expression there also appears to be an increased trend of hybrid fibers expressing both type I and type IIa myosin heavy chain (Thomason et al., 1986).

Non-weight bearing and single fiber contractile function

Stevens and Mounier (1992) utilized single skinned-fibers to study the effects of HS on SR function in rat soleus muscle. The authors reported that HS increased the sensitivity of SR calcium release to caffeine. The rate of calcium release, reuptake, and passive leakage from the SR all increased to levels resembling the fast plantaris muscle. These observations suggest that non-weight bearing may have a direct effect on the SR calcium release channel.

Decreases in absolute force (mN) of rat type I fibers following 7-14 days of HS range from 24-56% (Thompson et al., 1998; Widrick et al., 1996; McDonald et al., 1994) while normalized force (kN/m^2) decreases by 12-17% (Bangart et al., 1997; Widrick et al., 1996; Thompson et al., 1998; McDonald et al., 1994). The latter findings indicate that non-weight bearing affects the intrinsic ability of type I fibers to produce force because force decreases exceeded the amount of atrophy.

Maximal shortening velocities (V_o) of type I single fibers in rat soleus have also been reported to increase by 33% after 2 weeks of non-weight bearing (Widrick et al., 1996). The authors attributed the increased V_o to a reduction in the number of fibers with relatively low V_o and an increase in the number of single type I fibers displaying an increased V_o. Thompson et al. (1998) found that in rat soleus type I fibers, V_o increased by 56% after 1 week of HS compared with controls.

Increased V_o of type I fibers following non-weight bearing has also been reported in humans. Widrick et al. (1999) found that type I fibers in human soleus displayed an increased V_o of 30% following 17 days of space flight. The authors hypothesized that the increased V_o may have occurred due to the selective loss of thin filaments, which would be expected to increase the distance between thin and thick filaments (Riley et al., 2000). This structural change would result in an earlier detachment of the cross-bridge, which in turn would reduce the internal drag that develops during the final portion of the cross-bridge stroke.

Peak power is the product of the maximal shortening velocity (V_o) and peak tension (P_o). The decrease in peak tension in the soleus muscle results in a decrease in overall power even though the shortening velocity of the whole muscle and single fibers increases. The increased shortening velocity of whole soleus muscle and single fibers appear to act as a protective mechanism to minimize the decrease in muscle power caused by the substantial decreases in peak tetanic force with HS. Caiozzo et al. (1996) reported that peak power in whole muscle rat soleus was significantly reduced after 2 weeks of space flight. Similarly, McDonald et al. (1994) reported that after 1 and 2 weeks of HS, peak power ($\mu N \cdot FL \cdot s^{-1}$) of rat type I fibers decreased 18% and 49% respectively, while maximal shortening velocity increased and peak tension decreased at both time points.

Force production is regulated by calcium binding to the thin filament regulatory protein troponin. Calcium activation of force production involves a cooperative relationship that is fiber-type dependent (Gardetto et al., 1989). Slow

twitch muscle fibers have a lower calcium threshold for activation, and thus, require less calcium to reach active state. Non-weight bearing alters the dependence of force development on calcium concentration in soleus fibers, shifting the force-calcium concentration (force-pCa) curve to the right and increasing its steepness (McDonald and Fitts, 1995; Bangart et al., 1997; Gardetto et al., 1989). The right shift indicates that the fiber requires more calcium to become activated, i.e. there is a reduced sensitivity to calcium. An increase in the slope of the force-pCa curve indicates higher cooperative binding of calcium, which is a characteristic of fast fibers (Gardetto et al., 1989).

In summary, it appears that non-weight bearing causes severe atrophy of rat soleus type I fibers that is accompanied by decreased absolute and specific force production. Increases in soleus type I fiber V_o in rats and humans with non-weight bearing may act as a protective mechanism in order to reduce decreases in power that occur with decreased single fiber force production. Since type II fibers represent about 10% of the soleus muscle in rats and humans they are rarely studied with respect to their response to non-weight bearing. Thus, it is difficult to predict if type II fibers will respond in the same manner as type I fibers following non-weight bearing.

The mouse model in biomedical research

The mouse model has been used in biomedical research for centuries. In fact, Robert Hooke conducted the first documented experiments with mice in 1664 (Malakoff, 2002). In 1901, William Castle, who is considered the grandfather of mammalian genetics, was the first to realize the potential use of the mouse to test Mendel's genetic theories because of its small size, quick breeding, and recognizable variations. In 1909, Clarence Cooke Little bred 20 generations of brothers and sisters, and created the DBA (dilute, brown, and non-agouti) mouse strain, which was the first inbred strain. The DBA strain is considered to be the birth of the laboratory mouse.

Presently, there are over a 1000 different strains of mice available for research including 400 inbred strains (Malakoff, 2002). It is estimated that over 25 million mice will be raised this year, accounting for more than 90% of all mammals used in research (Malakoff, 2002). The mouse is well suited for biomedical research since it is one of the smallest mammals with adult weights of 25-40 grams, about 10-fold lighter than a rat. Their small size means that mice are more economical. Their housing costs are smaller because they require less space and their maintenance costs are smaller because they require less food. Mice also have a short generation time and are prolific breeders that can generate up to 250 descendants per year.

Perhaps the greatest advantage the mouse model provides is the fact that their genome has been thoroughly studied and is being sequenced. The mouse is the only other mammal besides humans that is scheduled for complete genetic sequencing. As of May 2002, 95% of the C57BL/6 mouse genome has been described and sequenced. Importantly, the mouse genome is easier to manipulate than other common laboratory species such as the rat (Tsika, 1994). It is clear that the use of gene knockout or protein over-expression models has the potential to greatly enhance our understanding of protein-function relationships.

There are many reasons that make the mouse model ideal for the study of the effects of non-weight bearing on muscle function. Considering that the cost of conducting experiments in space is $10,000 per kilogram of weight (Fejtek and Wasserburg, 1999), mice with their small size and maintenance cost are more economical research tools than the 10-fold heavier rat.

Unlike the rat and human models, the mouse soleus is a heterogeneous muscle with a mixed myosin heavy chain (MHC) composition. In fact, mouse soleus myosin heavy chain composition varies dramatically across strains and ranges from 35-75% type I (Haida et al., 1989; Wernig et al., 1990). The latter finding makes the mouse model intriguing for the study of non-weight bearing because it is possible to study the effects of non-weight bearing on soleus muscle function with a predominantly slow or fast muscle. This would allow researchers to examine the effects of non-weight bearing on fast and slow fibers from the antigravity soleus muscle, rather than studying slow fibers from the soleus and fast

fibers from muscles less affected by non-weight bearing, as is often done with rat studies. Finally, the use of transgenic and knockout mouse models may help researchers elucidate the mechanisms by which non-weight bearing affects muscle function.

Studies of single fiber contractile function with mice

There are only four studies that have conducted experiments on mouse skeletal skinned muscle fibers (Warren et al., 1994; Matsubara et al., 1985; Brooks and Faulkner, 1994; Seow and Ford, 1991). None of these studies have defined the relationship between single fiber contractile function and myosin heavy chain isoform expression. Thus, it is clear that data examining the relationship between single fiber contractile function and myosin heavy chain expression in the mouse is lacking.

Studies of non-weight bearing with mice

Despite the great potential the mouse model may have in enhancing our understanding of the effects on non-weight bearing on muscle function, there are few data on the effects of hindlimb suspension on mice. A possible reason for this may be due in part to the small size of their muscles. This presents a technical challenge for researchers. A typical mouse soleus can weigh between 7-10 mg and

even less after non-weight bearing, making it difficult to dissect and manipulate in studies of contractile function.

Generally, studies using mice report whole muscle atrophy that is similar to the rat following non-weight bearing. Following 7-14 days of HS the mouse soleus atrophies 24-45% (McCarthy et al., 1997; Steffen et al., 1984; Carlson et al., 1999; Ingalls et al., 1999) and the soleus to body mass ratio decreases 16-38% (Criswell et al., 1998a; Haida et al., 1989; Steffen et al., 1984; Ingalls et al., 1999). Other hindlimb muscles, such as the gastrocnemius and plantaris, atrophy 14-22% (Criswell et al., 1998b; Carlson et al., 1999; Steffen et al., 1984) following 7-14 days of HS. Thus, it appears that despite having a two-fold higher metabolic rate (Taylor et al., 1970) and a vastly different soleus myosin heavy chain composition, the time course and amount of atrophy in the mouse hindlimb muscles are similar to the rat.

Some studies have found that the mouse HS model is similar to the rat HS model, while others have reported differences. Warren et al. (1994) and Ingalls et al. (1999) found that 14 days of HS caused significant reductions in mouse soleus twitch tension (12-21%) while Haida et al. (1989) reported no change. Similarly, Warren et al. (1994) and Ingalls et al. (1999) reported that peak tetanic tension normalized for muscle cross-sectional area (CSA) decreased 15% and 24%, respectively, following 14 days of hindlimb suspension, while Haida et al. (1989) found no change. Haida et al. (1989) findings are difficult to interpret since the

soleus muscle did show significant atrophy and reduction in the ratio of soleus mass/body mass, indicating that a decrease in twitch tension would be expected.

Hindlimb suspension-induced changes in mouse muscle twitch properties have also been variable. Warren et al. (1994) reported that soleus half relaxation time and time to peak tension decreased 13% and 18%, respectively following 14 days of HS, while Haida et al. (1989) found no change. It is interesting to note that Haida et al. (1989) did not find that the proportion of fast type IIa myosin heavy chain increased in the soleus following HS, which might explain the lack of observed decrease in the latter two variables. Thus, some studies report that the mouse soleus shows faster shortening velocity following HS while others report no change.

An examination of the current literature on hindlimb suspension with mice suggests that whole muscle atrophy is similar to the rat. However, the few studies that have examined mouse soleus muscle contractile function following HS have showed variable results that are often difficult to interpret. Clearly there is a lack of knowledge with regard to the protein-function relationships in mouse single skeletal muscle fibers. Furthermore, there are no data on the effects of non-weight bearing on the contractile function of single cells in mice.

Overview of manuscripts in chapters 2-4

Although the mouse is the mammal most used in biomedical research, very little is known about protein-function relationships in single skeletal muscle cells in this species. Furthermore, despite the great potential that transgenic and knockout mouse models hold for elucidating the mechanisms that govern changes in muscle mass and function following non-weight bearing, there are only a few studies of non-weight bearing that have used mice. Since the mouse soleus muscle is heterogeneous in composition, whole muscle studies cannot effectively evaluate changes occurring in slow and fast fibers following non-weight bearing. Thus, it is important to assess the response of single muscle cells to non-weight bearing in the mouse model. In Chapter 2, the contractile function of all fiber types in mouse skeletal muscle was evaluated. The C57BL/6 strain was used for this study because it is the most commonly used inbred strain in biomedical research. The effect of myosin heavy chain isoform on fiber size, force production, and maximal shortening velocity was examined and compared to studies of single fiber function in other species. Our results will be useful to other researchers who study mouse muscle because they would have data on mouse skeletal muscle fiber function, which they can use to interpret their results. The manuscript presented in Chapter 3 extends the work completed in Chapter 2. The focus of this manuscript was to study the effects of 7 days of HS on the function of single muscle fibers from the C57BL/6 mouse soleus, the muscle that is most affected by non-weight bearing.

In humans and rats, the literature suggests that soleus slow type I fibers are more affected than fast type II fibers following non-weight bearing. Since the mouse soleus muscle is more heterogeneous in fiber composition, it is possible to study the effects of non-weight bearing on slow and fast fibers from the same muscle. Chapter 3 describes the response of slow and fast soleus fibers to 7 days of HS from C57BL/6 mice. These are the first data that examine changes in contractile function of mouse single skeletal muscle cells following HS. We found that in this strain, type I and type II fibers responded similarly to HS with respect to atrophy, and decreases in force. Surprisingly, unlike rat and human studies of non-weight bearing, we found no changes in maximal shortening velocity of type I fibers. The latter finding led to our last manuscript presented in Chapter 4, which examined the effects of 7 days of HS on contractile function of single skeletal muscle fibers from solei muscles of two strains (ICR and CBA/J) of mice that contain a higher composition of type I fibers, a composition more similar to those found in rats and humans.

In Chapter 4 we investigated the role soleus myosin heavy chain composition plays in the functional changes that type I and II fibers undergo following 7 days of HS. The contractile changes in type I and II fibers following 7 days of HS were similar to those found in the C57BL/6 strain with respect to fiber atrophy and decreases in force production, but were different with respect to changes in maximal shortening velocity. We found that changes in contractile function following non-weight bearing were related to the myosin heavy chain

composition of the soleus muscle. Both the ICR and CBA/J strains responded differently to non-weight bearing than the C57BL/6 strain.

These data have produced a significant advance in our understanding of protein-function relationships of single skeletal muscle fibers in mice. Our data from the HS studies challenge previous notions that soleus type I fibers are more susceptible than type II fibers following non-weight bearing, and instead suggest, that the response of soleus single muscle fibers to non-weight bearing is governed, in part, by the myosin heavy chain composition of the muscle.

Chapter 2

Protein-Function Relationships of Skinned Single Skeletal Muscle Fibers
from C57BL/6 Mice

Julian E. Stelzer and Jeffrey J. Widrick

Department of Exercise and Sport Science

Abstract

The mouse is the most widely used mammal in biomedical research today yet there are few data on the protein-function relationships of mouse skeletal muscle cells. Our aim was to establish these relationships by studying skinned muscle fibers prepared from soleus, gastrocnemius, and plantaris muscles of C57BL/6 mice using an in vitro single-cell preparation. The soleus muscle was found to contain a majority of fibers expressing fast myosin heavy chain (MHC) (20% type I, 78% type IIa, and type IIb 2%) while the plantaris, gastrocnemius, tibialis anterior, and extensor digitorum longus expressed a majority of type IIb MHC (83% to 100% type IIb, and 12% to 17% type IIx). Specific peak Ca^{2+}-activated force was similar in all fiber types and ranged from 116 to 120 kN/m^2. The relationship between fiber type MHC expression and maximal shortening velocity (V_0) was (from slowest to fastest shortening): type I < type IIa < type IIx/IIb < type IIb. The observed V_0 of the IIb fibers was in good agreement with the V_0 predicted for a mammal of this body mass, however, the V_0 observed for the type I fibers was 25% slower than predicted. In summary, we found the general relationships between soleus fiber force, V_0, and protein isoform expression similar to other mammals. However, in contrast to many mammals the C57BL/6 soleus is a predominantly fast muscle, containing slow fibers with a slower than expected V_0.

Introduction

It is estimated that over 25 million mice are raised for research purposes each year, accounting for over 90% of all the mammals used in biomedical research (Malakoff, 2000). The use of mice in research has doubled in the last decade (Malakoff, 2000) because mice offer several advantages over other common laboratory species. These advantages include lower initial cost, lower cost of maintenance, short reproduction cycle, and prolific breeding. Most importantly, the mouse pro-nucleus is technically easier to manipulate than that of the rat, making the mouse the species of choice for most gene-knockout or protein over-expression studies (Tsika, 1994). This ability to manipulate the genome allows for experimental modification of protein expression, and therefore, the ability to examine protein-function relationships in various organs, tissues, and cells.

The primary functional properties of skeletal muscle cells are force and shortening velocity. The former is a function of the number of actomyosin cross-bridges, which is normally proportional to cell cross sectional area (CSA). The latter is determined primarily by myosin heavy chain (MHC) isoform content (Reiser et al., 1985). Studies examining the relationships between cell protein isoform expression and function have been conducted primarily on rat (Gardetto et al., 1989; Widrick et al., 1996; Bottinelli et al., 1994), rabbit (Reiser et al., 1985; Sweeney et al., 1986), monkey (Widrick et al, 1997; Fitts et al., 1998) or human muscle fibers (Larsson and Moss, 1993). Thus, despite the growing use of the

mouse as a research model, relatively little is known about the protein-function relationships of mouse skeletal muscle cells.

Since muscle fiber function scales with species body mass (Rome et al., 1990), most of the information available today on the functional properties of mouse muscle cells has been extrapolated from data obtained from other species (Rome et al., 1990; Rome et al., 1992; Widrick et al., 1997). However, the validity of such extrapolation is questionable because of the wide physiological variability that exists in the 1000 known strains of mice in use today (Festing, 1997). For instance, the MHC composition of the mouse soleus has been reported to contain as little as 35% type I fibers (strain 129B6F$_1$/J: Haida et al., 1989) or up to as much as 75% type I fibers (strain CBA/J: Wernig et al., 1990). Furthermore, it is well established that different strains of mice differ in their response to drug therapy, susceptibility to disease, life expectancy, anatomy, and even psychological behavior (Festing, 1994; Liu and Gershenfeld, 2001).

Several groups have studied the contractile function of mouse single muscle fibers (Brooks and Faulkner, 1994; Matsubara et al., 1985; Warren et al., 1994; Seow and Ford, 1991), but none have established how function is related to MHC isoform expression. Thus, the primary purpose of this study was to determine the relationship between MHC protein isoform and contractile function in skinned single muscle fibers obtained from the mouse hindlimb. A secondary aim was to characterize MHC isoform expression in the major muscles of the lower limb. For

this study, we chose to study the C57BL/6 mouse because this strain is the most widely used of the 400 inbred strains available today (Maher, 2002).

Methods

<u>Animals and surgical procedures</u>

Seventeen male C57BL/6 mice, 8-12 weeks of age (body mass of 24.8 ± 0.7 grams) were obtained from Simonsen Laboratories and housed at the Oregon State University Animal Care Facility. The facility was maintained at 23°C with a 12:12 hour light-dark cycle. Animals were maintained on a standard diet of laboratory chow and water. After a minimum 7-day acclimation period, mice were anesthetized with an intraperitonal injection of pentobarbital sodium (40 mg/kg body mass) and the hindlimb muscles including the soleus, plantaris, gastrocnemius, tibialis anterior, and extensor digitorum longus were excised. The soleus, gastrocnemius, and plantaris from one hindlimb were used for the preparation of skinned single fibers. These muscles were immediately placed in relaxing solution (for composition, see below) where they were dissected longitudinally into smaller bundles.

The muscle bundles were placed in a skinning solution, consisting of 50% dissection solution and 50% glycerol, and stored at 4° C. This treatment chemically disrupts the sarcolemma and other membrane bound organelles. After 24 hours, samples were placed in fresh skinning solution and stored at -20°C for up to 3

weeks. Muscles excised from the other hindlimb were frozen in liquid nitrogen and stored at -80°C. These samples were used to determine myosin heavy chain (MHC) isoform distribution. Animals were then killed by pnemothorax.

Solutions

An iterative computer program (Fabiato, 1988) was used to determine the composition of the relaxing and activating solutions used for physiological studies. Stability constants used in the calculations were adjusted for the experimental conditions of this project (Fabiato, 1985). All solutions contained 7.0 mM EGTA, 14.5 mM creatine phosphate, 20.0 mM imidazole, 15 U·ml^{-1} creatine kinase, 4 mM Mg^{2+}-ATP, and 1 mM free Mg^{2+}. The relaxing and activating solutions contained a total free Ca^{2+} concentration of pCa 9.0 and pCa 4.5, respectively (where pCa = - log $[Ca^{2+}]$), which was adjusted with $CaCl_2$ (Calcium Molarity Standard, Corning Inc., Corning, NY). For both solutions, pH was adjusted to 7.0 with KOH and total ionic strength to 180 mM with KCl.

The dissection solution consisted of a cocktail of protease inhibitors in relaxing solution (Complete Mini EDTA-Free Protease Inhibitor tablets, Boehringer Mannheim, Indianapolis, IN). The skinning solution was composed of equal volumes of glycerol and dissection solution.

Single fiber experiments

Muscle bundles were transferred to relaxing solution where single fibers were carefully isolated. The ends of an isolated single fiber were attached to stainless steel troughs using 4-0 monofilament posts and 10-0 suture (Widrick, 2002). The troughs were suspended in small wells milled into a stainless steel plate. One trough was connected to an isometric force transducer (Model 400, Aurora Scientific, Aurora, Ontario) while the other was attached to a direct-current position motor (Model 308B, Aurora Scientific). Output from the transducer and motor were monitored on a digital oscilloscope (Model Integra 10, Nicolet Technologies, Madison, WI). Amplified signals were digitized (5 kHz), and interfaced to a personal computer by a data acquisition board (Model AT-MIO-16E, National Instruments, Austin, TX). A custom computer program (written in LabView, National Instruments, Austin, TX) was used to control data acquisition, storage, and analysis.

The plate was mounted on an inverted microscope (600X) (Olympus IX-70, Olympus America Inc., Melville, NY) allowing the investigator to view the fiber through glass panels making up the bottom of each chamber. Sarcomere length was adjusted to 2.5 μm using a calibrated ocular micrometer and 3-axis micromanipulators mounted to the motor and force transducer. The length of the fiber (FL) was attained by translating the fiber across the microscope's field of view using a digital micrometer attached to the mechanical stage of the microscope. To calculate fiber cross-sectional area (CSA), fiber width was read from the ocular

micrometer while the mounted fiber was briefly suspended in air (< 5 s). Fiber CSA was calculated from the width measurement assuming the fiber forms a cylinder in air (Metzger and Moss, 1987; Widrick, 2002). Three CSA measurements were made along the length of the fiber (at ~ 0.25, 0.50, and 0.75 of FL, with the fiber returned to relaxing solution between measurements) with the average taken as the fiber CSA. The temperature of the solutions was monitored by a thermocouple and maintained at 15°C throughout all experiments by Peltier cells in contact with the stainless steel plate.

Activation of fibers was accomplished by depressing and translating the stainless steel plate so that the fiber was transferred to an adjacent chamber containing activating solution. Unloaded shortening velocity (V_o) and peak Ca^{2+}-activated force (P_o) were determined using the slack test method (Edman, 1979; Widrick, 2002). In this procedure, the fiber is subjected to a series of slack steps and the time to force re-development is measured (Figure 2.1). A minimum of five different slack-step lengths, never greater than 20% of FL, were plotted against the corresponding times required for tension re-development and fit by a least squares linear regression (Figure 2.2). Unloaded shortening velocity, was taken as the slope of the regression line, and was normalized to the length of the fiber and expressed as FL/s. Peak Ca^{2+}-activated force was determined as the difference between the maximum force preceding the slack step and the force baseline obtained during unloaded shortening. Specific force was calculated by dividing peak isometric force by fiber CSA.
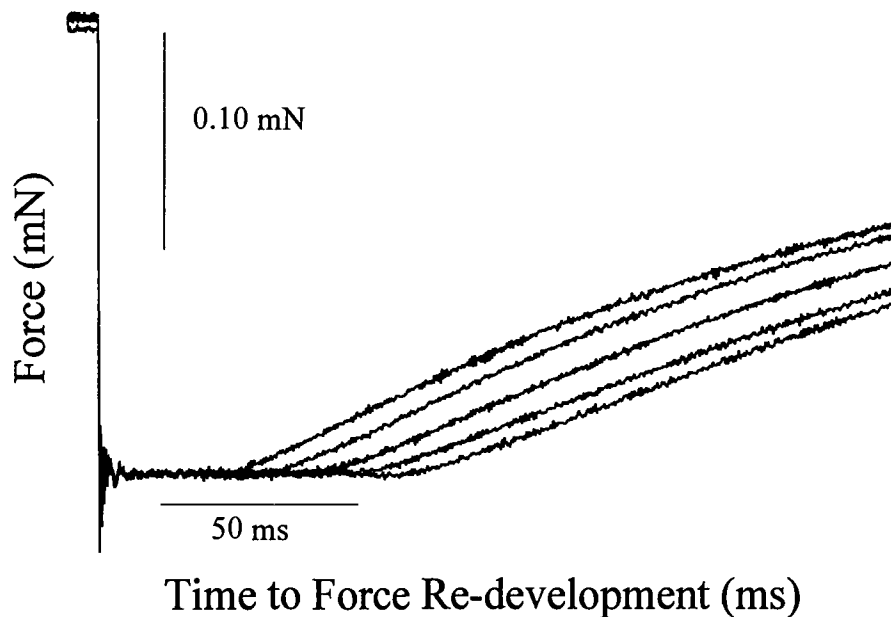
Figure 2.1 Force records obtained from 5 slack tests. The records have been superimposed. In each record the fiber was subjected to a rapid slack step length, causing force to drop to zero. The fiber shortened until it had taken up the slack, at which point there was a redevelopment of force. The fiber was relaxed, re-extended to its original fiber length, and subjected to another activation. During each subsequent activation, the distance of the slack step was increased, which resulted in a longer duration of unloaded shortening. The duration of unloaded shortening was plotted against the slack length as illustrated in Figure 2.2. Peak Ca^{2+}-activated force was determined as the difference in force immediately prior to the slack step and the force baseline during unloaded shortening.
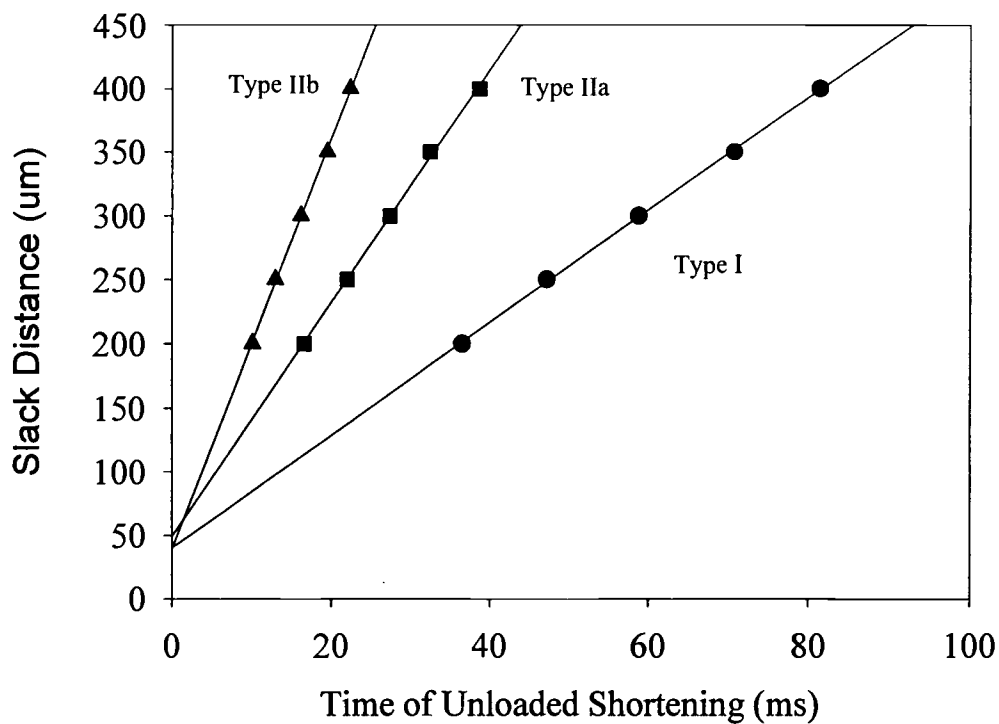
Figure 2.2 Slack distance versus time of unloaded shortening. A plot of the duration of unloaded shortening from 5 slack steps versus corresponding slack step length for fibers expressing type I (fiber from Figure 2.1), IIa, and IIb MHC, respectively. The slope of the first order least squares regression ($R^2 = 0.999$, respectively) fit to the data points represents the fibers unloaded shortening velocity. In this example the shortening velocity for the type I (●), IIa (■), and IIb (▲) fibers, was found to be 1.67 FL/s, 3.52 FL/s, and 6.55 FL/s, respectively.

Gel electrophoresis

At the end of each physiological experiment the fiber was removed from the troughs and stored in SDS sample buffer (containing 10% glycerol, 5% beta-mercaptoethanol, 2% SDS, 62.5 mM Tris (pH 6.8), and 0.001% bromophenol blue). The fiber was denatured for 4 minutes at 95°C, and stored at -80°C. To determine MHC composition, a sample of the fiber solute was later run on a discontinuous polyacrylamide gel system consisting of a 7% separating gel and a 3.5% stacking gel (Fauteck and Kandarian, 1995). Electrophoresis was carried out on a Bio-rad mini-Protean 3 electrophoresis system (Bio-Rad Laboratories, Hercules, CA) running at 70 V for 24 hours (4°C). Whole muscle MHC content was determined by extracting myosin from samples of mouse soleus, plantaris, tibialis anterior, extensor digitorum longus, and gastrocnemius muscles (LaFramboise et al., 1990) and running samples on similar gels. A silver staining procedure (Shevchenko et al., 1996) was used to visualize protein bands (Figure 2.3 and Figure 2.4).

Densitometry

Relative hybrid composition was assessed using laser-scanning densitometry (Molecular Dynamics, ImageQuaNT 5.0, Sunnyvale, CA). Gels were scanned for 100-micron pixel size and area integration was performed to determine relative density of each MHC band present in muscle samples or in fibers containing multiple MHC isoforms.

IIa
IIx ==
IIb
I —

A   B   C   D   E
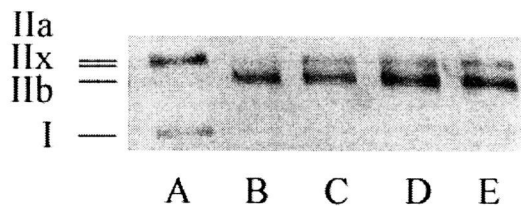
Figure 2.3 Silver stained gel electrophoresis procedure. Figure illustrates MHC isoform identification in muscle homogenates. Each lane contained a different homogenized hindlimb muscle. In this example lane A contained a soleus muscle, lane B gastrocnemius, lane C plantaris, lane D tibialis anterior, and lane E extensor digitorum longus. MHC isoform are from top to bottom: type IIa, IIx, IIb, and I.

IIa
IIx
IIb
I
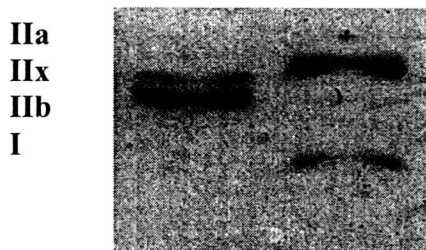
Figure 2.4 Soleus and plantaris MHC standards. Myosin heavy chain standards prepared from plantaris (left lane) and soleus (right lane) muscles. These standards illustrate the 4 MHC isoforms used to determine single fiber MHC content. Myosin heavy chain isoforms are from top to bottom: Type IIa, IIx, IIb, and I.

<u>Statistical analysis</u>

All data are reported as means ± SE. Statistical significance for all measures was determined with a one-way analysis of variance (ANOVA) combined with a Tukey's post hoc test. One-way ANOVA was run using type III sum of squares to account for unequal number of observations for each variable. Statistical significance was accepted as $p<0.05$. All statistics were computed using SPSS version 10.0 (SPSS Inc, Chicago, IL).

Results

<u>Distribution of MHC in hindlimb muscles</u>

Whole muscle MHC profiles are summarized in Table 2.1. Myosin extracted from soleus, plantaris, gastrocnemius, tibialis anterior, and extensor digitorum longus muscles was electrophoresed and the relative content of each isoform (I, IIa, IIx, and IIb) was determined by densitometry. The C57BL/6 soleus muscle was composed of a majority of fast MHC, primarily type IIa with a small amount of type IIb. Type I MHC made up only 20% of the total MHC in the soleus. The gastrocnemius muscle was comprised solely of type IIb myosin, while the plantaris, tibialis anterior, and extensor digitorum longus expressed a majority of type IIb MHC (at least 80%) with varying amounts of IIx MHC.

Table 2.1. MHC isoform percent distribution of selected hindlimb muscles of the C57BL/6 mouse

	Percent Distribution			
Muscle	MHC I	MHC IIa	MHC IIx	MHC IIb
SOL	19.9 ± 2.0	78.5 ± 2.0	nd	1.6 ± 1.6
PLT	nd	nd	17.5 ± 1.9	82.5 ± 1.9
GAST	nd	nd	nd	100.0
TA	nd	nd	15.4 ± 1.1	84.6 ± 1.1
EDL	nd	nd	11.8 ± 3.0	88.2 ± 3.0

Values are mean ± SE of 6-7 muscles. Percent MHC distribution of hindlimb muscles determined by densitometry. Abbreviations: SOL, soleus; PLT, plantaris; GAST, gastrocnemius; TA, tibialis anterior; EDL, extensor digitorum longus; MHC, myosin heavy chain; nd, not detected.

Fiber cross-sectional area and peak Ca^{2+}-activated force

Functional experiments were conducted on fiber segments isolated from the soleus, gastrocnemius, and the plantaris. These three muscles were selected because together, they contain all the MHC isoforms. However, despite isolating and studying single fiber segments from the gastrocnemius and plantaris, no fibers were found to express the pure IIx MHC isoform. Instead, type IIx was always found co-expressed with the type IIb isoform. For this reason no data are available for the type IIx MHC isoform. Since 402 (97%) of the 416 fibers studied expressed type I, type IIa, type IIx/IIb, and type IIb MHC, this paper focuses on these groups of fibers.

Fibers expressing type IIa MHC had the smallest CSA, while type I, type IIx/IIb, and IIb fibers, had CSA that were 10%, 66%, and 92% greater, respectively. The latter were significantly greater in CSA than all other fiber types (Table 2.2).

Peak isometric force (mN) was proportional to fiber CSA and was greatest in type IIb fibers due to their large size (Table 2.2). Type IIx/IIb, type I, and IIa fibers produced forces that were 11%, 38%, and 45% lower, respectively, than the IIb fibers. When peak isometric force was normalized for fiber CSA, all fiber types displayed similar specific force.

Table 2.2. CSA, P_o, and P_o/CSA, of skinned muscle fibers isolated from soleus, gastrocnemius, and plantaris muscles of C57BL/6 mice

MHC	n	CSA (μm^2)	P_o (mN)	P_o/CSA (kN/m^2)
I	43	1538 ± 54 [a]	0.19 ± 0.01 [a]	119 ± 2
IIa	155	1394 ± 35 [a]	0.17 ± 0.01 [a]	119 ± 1
IIx/IIb	44	2307 ± 69 [b]	0.28 ± 0.01 [b]	120 ± 2
IIb	160	2678 ± 62 [c]	0.31 ± 0.01 [b]	116 ± 1

Values are mean $\pm$ SE. Abbreviations: MHC, myosin heavy chain; n, number of fibers isolated from muscle bundles; CSA, cross-sectional area; P_o, peak isometric force; P_o/CSA, peak isometric force per cross-sectional area. Means with different superscripts are significantly different ($p<0.05$). Fibers were pooled from soleus, gastrocnemius, and plantaris muscles as follows: type I: soleus = 41, gastrocnemius = 2; type IIa: soleus = 134, gastrocnemius = 7, plantaris = 14; type IIx/IIb: soleus = 17, gastrocnemius = 3, plantaris = 25; type IIb: soleus = 4, gastrocnemius = 102, plantaris = 55.

<u>Unloaded shortening velocity</u>

There was a significant effect of MHC isoform expression on fiber V_o (Table 2.3). The relationship between fiber MHC expression was (from slowest to fastest shortening): type I < type IIa < type IIx/IIb < type IIb. Specifically, type IIa fibers were 2.32 fold faster on average than type I fibers, while type IIx/IIb, and IIb fibers were, 3.65, and 4.28 fold faster on average than type I fibers, respectively (Table 2.3).

Discussion

There are over 400 inbred mice strains available for research (Festing, 1997). A survey of the literature reveals that 10 strains are used in about 70% of all studies using inbred mice (Nishioka, 1995). The C57BL/6 mouse is the most widely used of all inbred strains with an estimated 14% share. Because it is anticipated that the use of mice in muscle physiology will increase (Malakoff, 2002), we examined the relationship between MHC isoform expression and contractile function in skinned single skeletal muscle fibers of the C57BL/6 mouse. In most larger mammals, including humans, rabbits, and rats, the soleus is comprised of 80-90% type I fibers (Reiser et al., 1985; Bottinelli et al., 1996; Delp and Duan, 1996). For this reason, the rat soleus is often used as a model of a slow muscle. Our results show that the soleus muscle of the C57BL/6 mouse is comprised of only 20% type I MHC. The predominant isoform expressed in the

Table 2.3. V_o of skinned muscle fibers isolated from soleus, gastrocnemius, and plantaris muscles of C57BL/6 mice

MHC	V_o (FL/s)
I	1.53 ± 0.08 [a]
IIa	3.55 ± 0.10 [b]
IIx/IIb	5.58 ± 0.22 [c]
IIb	6.55 ± 0.14 [d]

Values are mean ± SE. Number of fibers is the same as in Table 2.2. Abbreviations: MHC, myosin heavy chain; V_o, maximal shortening velocity; FL/s, fiber lengths per second. Means with different superscripts are significantly different (p<0.05).

soleus is actually IIa, accounting for 78% of all myosin. We also noted a very low expression of IIb MHC that accounted for 2% of total myosin. Thus, in this particular mouse strain, the soleus is a predominantly fast muscle rather than a predominantly slow muscle as in other common laboratory species. This is an important consideration in the design and interpretation of experiments that use this particular mouse strain.

A surprising amount of variability in mouse solei MHC isoform content has been reported in the literature. Most of these studies have used histochemical techniques which stain for fiber ATPase activity. Haida et al. (1989) reported that the mouse soleus was comprised of 35% type I fibers (strain 129B6F$_1$/J), Warren et al. (1994) reported 55% type I (strain ICR), and Wernig et al. (1990) reported 75% type I (strain CBA/J). Note that these data arise from different mouse strains. Coupled with the present data, which examined MHC isoforms, it seems that soleus fiber type composition is highly variable among mouse strains. The physiological purpose of the high inter-strain variability in the soleus muscle fiber composition is unclear. However, the general assumption that the mouse soleus represents a classic slow muscle is not valid.

The MHC compositions of the other hindlimb muscles from the C57BL/6 mouse are consistent with the reported literature in mice (Carlson et al., 1999; Zardini and Parry, 1994; Hämäläinen et al., 1993). We found the gastrocnemius muscle to be almost exclusively comprised of type IIb MHC, while the extensor digitorum longus, plantaris, and tibialis anterior, are comprised of a majority of

type IIb MHC with a range of 15-35% type IIx MHC. Our findings are in agreement with findings that type IIb myosin make up 77% of the mouse hindlimb (Agbulut et al., 1996) and consistent with the idea that there is an inverse relationship between body mass and type IIb MHC expression in mammals (Sartorius et al., 1998).

It is interesting to note that no fibers expressed the type IIx MHC exclusively. Rather, IIx was co-expressed with type IIb MHC. The role of the IIx MHC population is yet unclear, but studies of mice devoid of type IIx MHC have shown that the type IIx MHC represents a distinct population with a significant functional role (Sartorius et al., 1998).

In the present study we did not find physiologically significant differences in the intrinsic ability of fibers expressing different MHC isoforms to produce force. When absolute force was normalized to fiber CSA the force produced by each fiber type was virtually identical. The average specific tension observed in all fibers ranged from 116-120 $kN/\mu m^2$ regardless of isoform which is similar to specific tension reported in rats (Gardetto et al., 1989; Bottinelli et al., 1994) humans (Bottinelli et al., 1996; Widrick et al., 1999), and mice (Brooks and Faulkner, 1994). This finding is in agreement with Widrick et al. (1997) and Rome et al. (1990) who found that fiber-specific tension (peak force/fiber cross sectional area) for slow and fast fibers is essentially independent of species body mass.

Most studies conducted in larger mammals, such as humans, have found that fibers expressing faster MHC isoforms produce more specific force than fibers

expressing slow MHC isoforms (Widrick et al., 2002; Bottinelli et al., 1996; Frontera et al., 2000). These differences appear to exist in the rat as well although they are sometimes less pronounced (Gardetto et al., 1989; Rome et al., 1990). It has been suggested that the difference in intrinsic force production of different fiber types is due to the higher density of myosin in fast versus slow fibers (Tikunov et al., 2001). It is possible that in the mouse the differences in fiber myosin concentration are not substantial enough to significantly affect force production.

As expected, fibers expressing type I MHC had the slowest shortening velocity while fibers expressing type IIb MHC had the fastest. There are two studies in the literature that have examined shortening velocity of mice fibers (Brooks and Faulkner, 1994; Seow and Ford, 1991). However, comparison of our results to these studies is confounded by the fact that neither study determined fiber MHC isoform content. Brooks and Faulkner (1994) reported a V_0 of 6.42 FL/s for C57BL/6 mouse extensor digitorum longus fibers. This is similar to our value of 6.55 FL/s for fibers expressing type IIb MHC and is consistent with our finding that type IIb MHC represents 88% of the total C57BL/6 extensor digitorum longus fiber population. Seow and Ford (1991) performed their experiments at 5°C instead of 15°C and they determined maximal shortening velocity by extrapolation of force-velocity curves. Assuming a Q_{10} temperature factor of 2 (Pate et al., 1994), Seow and Ford's (1991) fast fiber V_0 taken from the extensor digitorum longus was 30% lower than our type IIb V_0. However, the shortening velocity of fast fibers obtained from force-velocity curves tends to underestimate V_0 obtained by the slack test

method (Bottinelli et al., 1996). Thus, our data appear reasonably similar to the results of Seow and Ford (1991).

Rome et al. (1990) predicted, based on a body mass scaling model, that type IIb fiber V_o would be 6.56 FL/s for a 25-gram mammal. Our type IIb fiber V_o is in agreement with this prediction (Figure 2.5). Rome et al. (1990) and Widrick et al. (1997) predicted that the maximal shortening velocity of fibers expressing type I MHC would be between 1.92 FL/s (Figure 2.5) and 2.33 FL/s for a 25-gram mammal, respectively. Note in Figure 2.5 that this predicted type I fiber V_o is 25-50% higher than the average value observed in the present study (1.53 FL/s).

The similarity between the predicted type IIb fiber V_o and the observed value suggests that the lower than expected V_o of the type I fibers is not due to a experimental artifact or systematic effect that lowered all V_o values. This raises the question why type I fibers from C57BL/6 mice have slower than expected V_o. The predicted values from Rome et al. (1990) and Widrick et al. (1997) are extrapolations, since neither study examined fibers from mammals smaller than laboratory rats. However, it is interesting to note that the type IIb V_o regression equation derived from fast muscles which show little MHC content variation across species matched our data. Prediction models of slow fiber V_o are derived from mammals that contain a typically high type I fiber soleus muscle composition (rat, rabbit, human). The C57BL/6 mouse soleus has a small population of type I fibers. Thus, one possibility is that the present data do not fit the predicted values because
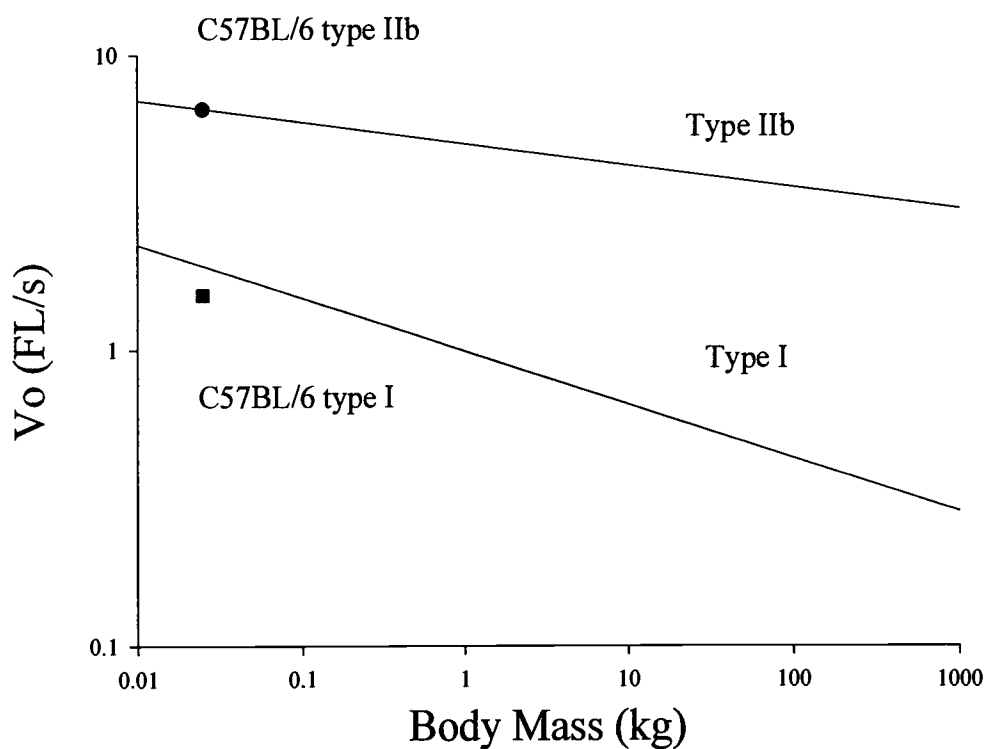
Figure 2.5 Shortening velocity regression equations. Log of shortening velocity versus log of animal body mass. Type I (bottom line) and IIb (top line) regression lines taken from Rome et al. (1990) showing the predicted effect of decreasing body mass on fiber shortening velocity. Average shortening velocity of type IIb fibers (● top line) and type I fibers (■ bottom line) found in the present study.

of the substantially different fiber compositions of the C57BL/6 mouse and other small mammals.

It is possible that differences in soleus MHC isoform composition are related to discrepancies in type I shortening velocity. Marechal and Beckers-Bleukx (1993) found that the maximal shortening velocity of the soleus muscle from the NMRI mouse strain, which is comprised of 65% type I fibers, and the soleus from the C57BL/10 mouse strain, which they report contained 36% type I fibers, were similar. This suggests that the shortening velocity of the entire soleus is important, with differences in global MHC isoform distribution potentially offset by differences in the intrinsic shortening velocity of individual muscle fibers.

In summary, our data show that single fibers from the C57BL/6 mouse hindlimb display similar specific force values as fibers from other mammals. However, unlike other mammals, there is no physiologically significant difference in the intrinsic ability of fibers expressing different MHC isoforms to produce force. The shortening velocity of fast fibers in this mouse strain appears to agree with values previously reported in the literature, however, the shortening velocity of slow fibers is slower than predictions based on allometric scaling models. A possible reason for this deviation may be due to the unusually low composition of slow fibers in the predominantly fast C57BL/6 mouse soleus, which necessitates the slow fibers to shorten at slower velocities in order to maintain whole muscle function.

Chapter 3

Functional Responses of C57BL/6 Mouse Soleus Muscle Fibers to 7 Days of
Hindlimb Suspension

Julian E. Stelzer and Jeffrey J. Widrick

Department of Exercise and Sport Science

Abstract

Identifying mechanisms underlying skeletal muscle atrophy may be facilitated by a transition from rat to mouse hindlimb suspension (HS) models because of the availability of genetically modified mice. We tested whether mouse soleus muscle fibers would show functional adaptations to HS similar to those previously reported for soleus rat fibers. In C57BL/6 mice, 7 days of HS reduced soleus mass 25% and soleus fiber cross-sectional area 16-38%. Peak Ca^{2+}-activated force (P_o) was reduced 44-47% in skinned fibers expressing type I, IIa, or hybrid (I/IIa, IIa/IIb) myosin heavy chains (MHC); up to half of this decline was attributed to reductions in fiber specific force. HS had no effect on the soleus MHC profile (20-21% type I, 76-77% IIa, 2-3% IIb), the MHC isoform distribution of single soleus fibers, or the unloaded shortening velocity (V_o) of type I, IIa, or hybrid fibers. HS-induced soleus fiber atrophy and reductions in fiber P_o are similar for the C57BL/6 mouse and the rat. However, the C57BL/6 soleus is resistant to those changes in MHC isoform content and fiber V_o observed in the rat HS model. This suggests that the C57BL/6 mouse model of HS is not completely equivalent to the rat HS model.

Introduction

Hindlimb suspension (HS) is the most commonly used animal model of musculoskeletal non-weight bearing. The HS model was developed in the late 1970's as a ground-based model to mimic the effects of space flight on muscle function and bone metabolism. The model originally used laboratory rats (Musacchia et al., 1980; Morey, 1979) and most HS studies since have used this species (for review, see Thomason and Booth, 1990).

The rat soleus, which is comprised of about 90% slow, type I fibers, loses up to 40% of its mass after 7 days of HS (Thompson et al., 1998; Fitts et al., 1986). In addition to atrophy, HS induces a shift in the myosin heavy chain (MHC) composition of the soleus, resulting in a decreased expression of type I MHC, an increased expression of type IIa MHC, and de novo expression of type IIx MHC (Talmadge et al., 1996; Caiozzo et al., 1998; Caiozzo et al., 1997).

Only a limited number of studies have examined the responses of other common laboratory species to HS. These species have included hamsters (Corley et al., 1984), rabbits (Anzil et al., 1991), and mice (Haida et al., 1989; Warren et al., 1994; Ingalls et al., 2001). Mice, the most widely used species in biomedical research (Malakoff, 2000), offer several advantages over other animal models. Mice are smaller and therefore more economical to maintain than other laboratory species. Since the current cost of conducting research aboard the Space Shuttle is $10,000 per kg of weight (Fejtek and Wasserburg, 1999), the mouse, with a body

mass 10-fold smaller than that of the rat, makes for a more economical in-space model. However, the greatest advantage in using mice is the availability of, or the potential to produce, genetically modified animals. The use of transgenic and knockout mice will likely be important tools in elucidating the mechanisms involved in the response of skeletal muscle to conditions of non-weight bearing.

Mice have inherent characteristics that may elicit different responses to non-weight bearing than the rat. For instance, mice have a two-fold higher metabolic rate than rats (Taylor et al., 1970) and this could lead to greater atrophy with HS. Mice have also been shown to have distinctly different single fiber contractile function that rats (Seow and Ford, 1991). Unlike the rat, the mouse soleus is a mixed muscle, with a slow to fast fiber ratio varying from 20:80 to 75:25 depending on strain (Stelzer and Widrick, 2002; Wernig et al., 1990). This fiber heterogeneity may complicate the interpretation of the response of the soleus muscle to HS (Warren et al., 1994; Haida et al., 1989; Ingalls et al., 2001) since in the rat, slow and fast muscle fibers respond differently to HS (Gardetto et al., 1989).

The purpose of this study was to assess the changes in functional properties of slow and fast muscle fibers from the mouse soleus following 7 days of HS. The C57BL/6 strain of mouse was chosen for this study because it is the most widely used of all 400 inbred strains available for biomedical research today (Maher, 2002).

Methods

Animal care and suspension procedure

All protocols were approved by the Oregon State University Institutional Animal Care and Use Committee (IACUC). Male C57BL/6 mice (8-12 weeks old) were obtained from Simonsen Laboratories, acclimated for a 7-day period at Oregon State University's Animal Care Facility, and then randomly assigned to the hindlimb suspension (HS, n=11) or weight bearing control group (WB, n=17). Both groups were maintained on a similar diet of laboratory chow (ad libitum) and tap water. Animals were housed at 23°C with a 12:12 hour light-dark cycle.

The experimental mice were suspended by their tails for 7 days using a tail harness. A base layer of adhesive tape was glued to the proximal two-thirds of the tail with cyanoacrylate glue. An 18-gauge wire, shaped into a triangle, was attached to the base tape with additional strips of adhesive tape. The wire was positioned so its apex pointed upward, where a fish line swivel was clipped to the wire. Monofilament line was tied to the fish line swivel and used to raise the hindlimbs. The monofilament line was passed through a small hole in a sheet of Plexiglas that formed the 'roof' of the suspension apparatus. The length of the line was adjusted to prevent the hindlimbs from touching supportive surfaces. The forelimbs maintained contact with a grid floor, which allowed the animals to move about to feed. Waste passed through the grid onto absorbent paper. The exposed tip of the tail was monitored daily to ensure adequate blood flow.

Surgical procedures

Mice were anesthetized with an intraperitoneal injection of pentobarbital sodium (40 mg/kg body mass). The non-weight bearing mice were anaesthetized while still suspended in order to prevent any reloading-induced muscle damage. The left soleus was excised and used for the preparation of skinned single fibers (see below). The right hindlimb muscles, including the soleus, plantaris, gastrocnemius, tibialis anterior, and extensor digitorum longus, were removed, trimmed of connective tissue and fat, weighed, and frozen in liquid nitrogen. These samples were stored at -80°C, and later used for the determination of whole muscle myosin heavy chain (MHC) isoform distribution.

Tissue preparation

Immediately following dissection the excised left soleus muscle was placed in relaxing solution (for composition, see below) where it was dissected longitudinally into 2 or 3 bundles. The muscle bundles were transferred to a skinning solution, consisting of 50% dissection solution and 50% glycerol (for composition see below), and stored at 4°C. This treatment chemically permeabilized the sarcolemma and other membrane bound organelles. The skinning solution was replaced with new skinning solution after 24 hours, and samples were stored at -20°C for up to 4 weeks.

Solutions

The computer program of Fabiato (1988) was used to determine the composition of the relaxing and activating solutions used for physiological experiments. Stability constants used in these calculations were adjusted for the experimental conditions of this project (Fabiato, 1985). Relaxing and activating solutions contained 7.0 mM EGTA, 14.5 mM creatine phosphate, 20.0 mM imidazole, 15 U·ml^{-1} creatine kinase, 4 mM Mg^{2+}-ATP, and 1 mM free Mg^{2+}. KCl and KOH were used to adjust the total ionic strength to 180 mM and the pH to 7.0. The concentrations of free Ca^{2+} were 10^{-9} M and 10$^{-4.5}$ in the relaxing and activating solutions, respectively, and were expressed as pCa 9.0 and pCa 4.5 (where pCa = -log [Ca^{2+}]). The free Ca^{2+} concentrations were adjusted with CaCl$_2$ (Calcium Molarity Standard, Corning Inc., Corning, NY).

The dissection solution consisted of relaxing solution and a cocktail of protease inhibitors (Complete Mini EDTA-Free Protease Inhibitor tablets, Boehringer Mannheim, Indianapolis, IN). The skinning solution was composed of equal volumes of dissection solution and glycerol.

Single fiber experiments

Single fibers were isolated from muscle bundles while in relaxing solution using fine forceps. The ends of an isolated single fiber were secured to stainless steel troughs using 4-0 monofilament posts and 10-0 suture (Widrick, 2002). The right trough was connected to stationary isometric force transducer (Model 400,

Aurora Scientific, Aurora, Ontario) and the left to the lever arm of a direct-current position motor (Model 308B, Aurora Scientific). The troughs were suspended above wells milled into a stainless steel plate so that the fiber could be submerged in relaxing or activating solution. Output from the motor and transducer were monitored on a digital oscilloscope (Model Integra 10, Nicolet Technologies, Madison, WI). The signals were amplified, digitized (5 kHz), and interfaced to a personal computer by a data acquisition board (Model AT-MIO-16E, National Instruments, Austin, TX). Data acquisition, storage, and analysis were controlled through a custom computer program (written in LabView, National Instruments, Austin, TX).

An inverted microscope (600X) (Olympus IX-70, Olympus America Inc., Melville, NY) mounted underneath the steel plate was used to view the fiber through the transparent bottom of the chamber. An ocular micrometer and 3-axis micromanipulators were used to adjust the fiber sarcomere length to 2.5 μm. Fiber length (FL) was determined using a digital micrometer. Fiber cross-sectional area (CSA) was calculated by measuring the diameter of the fiber while it was briefly suspended in air under the assumption that the fiber forms a cylinder in air (Metzger and Moss, 1987; Widrick, 2002). Three measurements were taken along the length of the fiber with the average taken as the CSA.

Fiber activation was achieved by depressing the steel plate and transferring the fiber from the chamber containing relaxing solution to the chamber containing activating solution. Unloaded shortening velocity (V_o) and peak Ca^{2+}-activated

force (P_o) were determined using the slack test method (Edman, 1979; Widrick, 2002). The procedure involved subjecting the fiber to a minimum of five different slack steps ($\leq20\%$ FL) and measuring time to force re-development. Slack distances versus time to force re-development were plotted and fit by a least squares linear regression. The slope of the regression line normalized to FL was determined to be the unloaded shortening velocity (FL/s). Peak Ca^{2+}-activated force was determined as the difference between the maximum force achieved before the fiber was slacked and the baseline force acquired during unloaded shortening. Specific force was calculated by dividing peak isometric force by fiber CSA. Temperature was maintained at 15°C throughout all experiments using a series of Peltier cells in contact with the plate. Temperature was monitored by a thermocouple inserted into the experimental chamber.

Gel electrophoresis

At the end of each functional experiment, the single fiber was removed from the troughs and placed in 30 μl of SDS sample buffer. The sample buffer contained 10% glycerol, 5% beta-mercaptoethanol, 2% SDS, 62.5 mM Tris (pH 6.8), and 0.001% bromophenol blue. Prior to storage at -80°C, the fiber was denatured at 95°C for 4 minutes. MHC composition of each fiber was determined by loading a 2 μl sample of the solubilized fiber on a discontinuous polyacrylamide gel system consisting of a 7% separating gel and a 3.5% stacking gel (Fauteck and Kandarian, 1995). Electrophoresis was carried out on a Bio-rad mini-Protean 3

electrophoresis system (Bio-Rad Laboratories, Hercules, CA) running at 70 V for 24 hours (4°C). Myosin heavy-chain content of whole muscles was determined by extracting myosin from samples of mouse soleus, gastrocnemius, plantaris, tibialis anterior, and extensor digitorum longus muscles (LaFramboise et al., 1990) and running samples on similar gels. A silver staining procedure (Shevchenko et al., 1996) was used to visualize protein bands.

Densitometry

Relative hybrid composition was assessed using laser-scanning densitomery (Molecular Dynamics, ImageQuaNT 5.0, Sunnyvale, CA). Gels were scanned for 100-micron pixel size and area integration was performed to determine relative density of each MHC band present in muscle samples or in fibers containing multiple MHC isoforms.

Statistical analysis

Mean values for WB and HS groups were analyzed with a one-way analysis of variance. Statistical significance was accepted as $p<0.05$. All statistics were computed using SPSS version 10.0 (SPSS Inc, Chicago, IL).

Results

Body and soleus weight changes with HS

There was no significant difference in the body mass of WB (24.4 ± 0.7

grams) or 7-day HS (23.7 ± 0.9 grams) animals. Following HS there was a 25%

decrease in soleus wet weight and a 22% decrease in soleus muscle weight to body

weight ratio (Table 3.1). HS also caused atrophy of the gastrocnemius (22%),

plantaris (17%), and tibialis anterior (11%), but not the extensor digitorum longus.

MHC isoform expression

Soleus muscles from WB (n=8) and HS (n=8) animals contained 20% and

22% type I MHC, respectively. The remaining MHC consisted almost entirely of

the IIa isoform although there were small, but detectable levels of the IIb isoform

(Table 3.2). Similarly, MHC isoform composition of skinned WB (n=507) and HS

(n=560) fibers revealed that 17 ± 2% and 19 ± 2% of the fibers expressed type I

MHC (Table 3.3). Again, the remainder of the skinned soleus fibers expressed the

type IIa MHC isoform (WB: 68%; HS: 69%), a combination of type I and IIa

isoforms (WB: 4%; HS: 6%), and combinations of fibers expressing the IIb isoform

with the IIa or IIx isoform (WB: 10%; HS: 6%). The small population of fibers

expressing the IIx MHC isoform was not detected in the whole muscle homogenate

analysis. These results from whole muscle homogenates and single fibers indicated

that there was no shift in MHC distribution of type I ($p > 0.05$) and IIa ($p > 0.05$)

Table 3.1. Effect of 7 days of HS on hindlimb muscle weights of C57BL/6 mice

Muscle	Treatment	n	Muscle Mass (mg)	Muscle mass/BM
SOL	WB	17	9.2 ± 0.4	0.374 ± 0.009
	HS	11	6.9 ± 0.4*	0.292 ± 0.014*
PLT	WB	8	18.7 ± 0.6	0.711 ± 0.026
	HS	8	15.5 ± 0.8*	0.624 ± 0.031
GAST	WB	8	153.5 ± 2.8	5.853 ± 0.130
	HS	8	119.4 ± 2.2*	4.810 ± 0.107*
TA	WB	8	50.4 ± 0.9	1.919 ± 0.037
	HS	8	44.7 ± 1.5*	1.795 ± 0.045
EDL	WB	8	11.8 ± 0.4	0.451 ± 0.017
	HS	8	11.7 ± 0.8	0.468 ± 0.023

Values are mean ± SE. Abbreviations: WB, weight bearing; HS, hindlimb suspended; n, number of muscles; SOL, soleus; PLT, plantaris; GAST, gastrocnemius; TA, tibialis anterior; EDL, extensor digitorum longus; muscle mass/BM, muscle mass/body mass. Asterisk denotes significant difference from WB ($p<0.05$). PLT, GAST, TA, and EDL muscles were obtained from 8 WB and 8 HS animals. SOL muscles were obtained from an additional 6 WB and 3 HS animals.

Table 3.2. Effect of 7 days of HS on MHC composition of hindlimb muscles of C57BL/6 mice

Muscle	Treatment	Percent Distribution			
		MHC I	MHC IIa	MHC IIx	MHC IIb
SOL	WB	20.4 ± 1.7	77.1 ± 1.7	nd	2.5 ± 1.3
	HS	21.4 ± 2.0	75.6 ± 3.4	nd	3.0 ± 2.0
PLT	WB	nd	nd	16.3 ± 1.9	83.7 ± 1.9
	HS	nd	nd	16.3 ± 2.3	83.7 ± 2.3
GAST	WB	nd	nd	nd	100.0 ± 0.0
	HS	nd	nd	nd	100.0 ± 0.0
TA	WB	nd	nd	15.0 ± 1.3	85.0 ± 1.3
	HS	nd	nd	17.7 ± 1.4	82.3 ± 1.4
EDL	WB	nd	nd	12.5 ± 3.5	87.5 ± 3.5
	HS	nd	nd	11.1 ± 2.3	88.9 ± 2.3

Values are mean ± SE of 6-8 muscles. Percent distribution of MHC isoform of muscles was determined by densitometry. Abbreviations: WB, weight bearing; HS, hindlimb suspended; SOL, soleus; PLT, plantaris; GAST, gastrocnemius; TA, tibialis anterior; EDL, extensor digitorum longus; MHC, myosin heavy chain; nd, not detected. There were no statistically significant differences in the MHC composition of any muscle before and after HS.

Table 3.3. MHC fiber distribution of skinned fibers from C57BL/6
mice solei with or without HS

	Percent Distribution	
MHC Isoform	WB	HS
I	17 ± 2	19 ± 2
I/IIa	4 ± 2	6 ± 2
I/IIa/IIb	<1 ± 2	<1 ± 2
IIa	68 ± 5	69 ± 4
IIa/IIb	2 ± 3	3 ± 3
IIx/IIb	8 ± 3	3 ± 4
IIb	1 ± 3	nd

Values are percent of 100% ± SE. MHC isoform of skinned fibers determined by
gel electrophoresis. Abbreviations: MHC, myosin heavy chain; WB, weight
bearing; HS, hindlimb suspended; nd, not detected. Total of 1067 skinned fibers
(WB: n=507, HS: n=560). There were no statistically significant differences in any
MHC isoform percent distribution for WB and HS groups.

fibers after 7 days of HS. Similarly, HS did not alter the MHC distribution of the gastrocnemius, plantaris, tibialis anterior, or extensor digitorum longus (Table 3.2).

Fiber CSA and peak Ca^{2+}-activated force

A total of 412 fibers were included in the contractile function analysis: 212 from the WB animals and 200 from 7-day HS animals. Since 93% of the WB fibers and 97% of the HS fibers expressed type I, I/IIa, IIa, or IIx/IIb MHC isoform, our analysis focuses on these groups of fibers. No data are presented for the small number of fibers expressing type IIa/IIb (WB: n=10; HS: n=5) or type IIb (WB: n=4; HS: n=2).

HS caused significant atrophy of all fiber types with the greatest decreases occurring in type I/IIa fibers (38%) followed by type I and type IIa fibers (33%), and type IIx/IIb (16%) fibers (Table 3.4). When fibers were activated directly by Ca^{2+} we observed a substantial decrease in P_0 following HS for all fiber types (33-47%). The decline in force exceeded the decrease in fiber CSA (i.e. reduction in P_0/CSA) in all cases indicating a reduction in the intrinsic force producing mechanisms of the cell.

Unloaded shortening velocity

Fiber V_0 was highly dependent on MHC isoform content and could be described as type I < I/IIa < IIa < IIx/IIb (Table 3.5). This pattern was maintained after 7 days of HS since V_0 was unaltered for all fiber types. Type I V_0 -frequency

Table 3.4. Effect of 7 days of HS on fiber CSA, P_o, and P_o/CSA of soleus
type I, I/IIa, IIa, and IIx/IIb fibers of C57BL/6 mice

MHC	Treatment	n	CSA (μm^2)	P_o (mN)	P_o/CSA (kN/m^2)
I	WB	40	1519 ± 57	0.19 ± 0.01	119 ± 2
	HS	44	1015 ± 40*	0.10 ± 0.01*	101 ± 2*
I/IIa	WB	7	1430 ± 133	0.16 ± 0.01	114 ± 4
	HS	11	886 ± 103*	0.09 ± 0.01*	98 ± 7
IIa	WB	134	1370 ± 37	0.17 ± 0.01	120 ± 1
	HS	126	922 ± 27*	0.09 ± 0.01*	96 ± 1*
IIx/IIb	WB	17	2142 ± 104	0.27 ± 0.02	126 ± 3
	HS	12	1791 ± 138*	0.18 ± 0.01*	104 ± 4*

Values are mean $\pm$ SE. Abbreviations: MHC, myosin heavy chain; WB, weight
bearing; HS, hindlimb suspended; n, number of fibers; CSA, cross-sectional area;
P_o, peak isometric force; P_o/CSA; peak isometric force per cross-sectional area.
Asterisk denotes significant difference from WB ($p<0.05$).

Table 3.5. Effect of 7 days of HS on fiber V_o of soleus type
I, I/IIa, IIa, and IIx/IIb fibers of C57BL/6 mice

MHC	Treatment	V_o (FL/s)
I	WB	1.52 ± 0.08
	HS	1.56 ± 0.08
I/IIa	WB	3.12 ± 0.31
	HS	2.66 ± 0.34
IIa	WB	3.54 ± 0.11
	HS	3.43 ± 0.10
IIx/IIb	WB	5.58 ± 0.25
	HS	4.78 ± 0.36

Values are mean $\pm$ SE. Number of fibers is the same as Table 3.4. Abbreviations: WB, weight bearing; HS, hindlimb suspended; MHC, myosin heavy chain; V_o, maximal shortening velocity; FL/s, fiber lengths per second. There were statistically significant changes in V_o following HS for any fiber type.

histograms for WB and HS fibers show that there was no change in the V_o distribution of type I fibers following hindlimb suspension (Figure 3.1).

Discussion

The vast majority of studies examining the effects of non-weight bearing on muscle contractile function have been conducted on rats (Fitts et al., 1986; Gardetto et al., 1989; Thompson et al., 1998; McDonald e al., 1994; Ohira et al., 1992; Caiozzo et al., 1996) or humans (Widrick et al., 1999; Edgerton et al., 1995; Larsson et al., 1996; Riley et al., 1998; Andersen et al., 1999; Zhou et al., 1995; Adams et al., 1994). The few studies conducted on mice (Ingalls et al., 2001; Ingalls et al., 1999; Warren et al., 1994; Haida et al., 1989) have focused on whole muscle function rather than cellular mechanisms of contraction. Mice subjected to 7 days of HS show soleus muscle atrophy (Steffen et al., 1984; Criswell et al., 1998a; Ingalls et al., 2001; Carlson et al., 1999), and reductions in tetanic force and in force/muscle CSA (Haida et al., 1989; Steffen et al., 1984; Ingalls et al., 2001). Our data suggest that despite having a 2-fold higher resting metabolic rate (Taylor et al., 1970), and radically different MHC profile, the time course and the amount of gross atrophy in the mouse soleus muscle are similar to the rat. Our single fiber experiments extend these findings to the cellular level.

The unique aspect of the present study is its focus on the effects of non-weight bearing on the contractile function of mouse soleus single muscle fibers. We
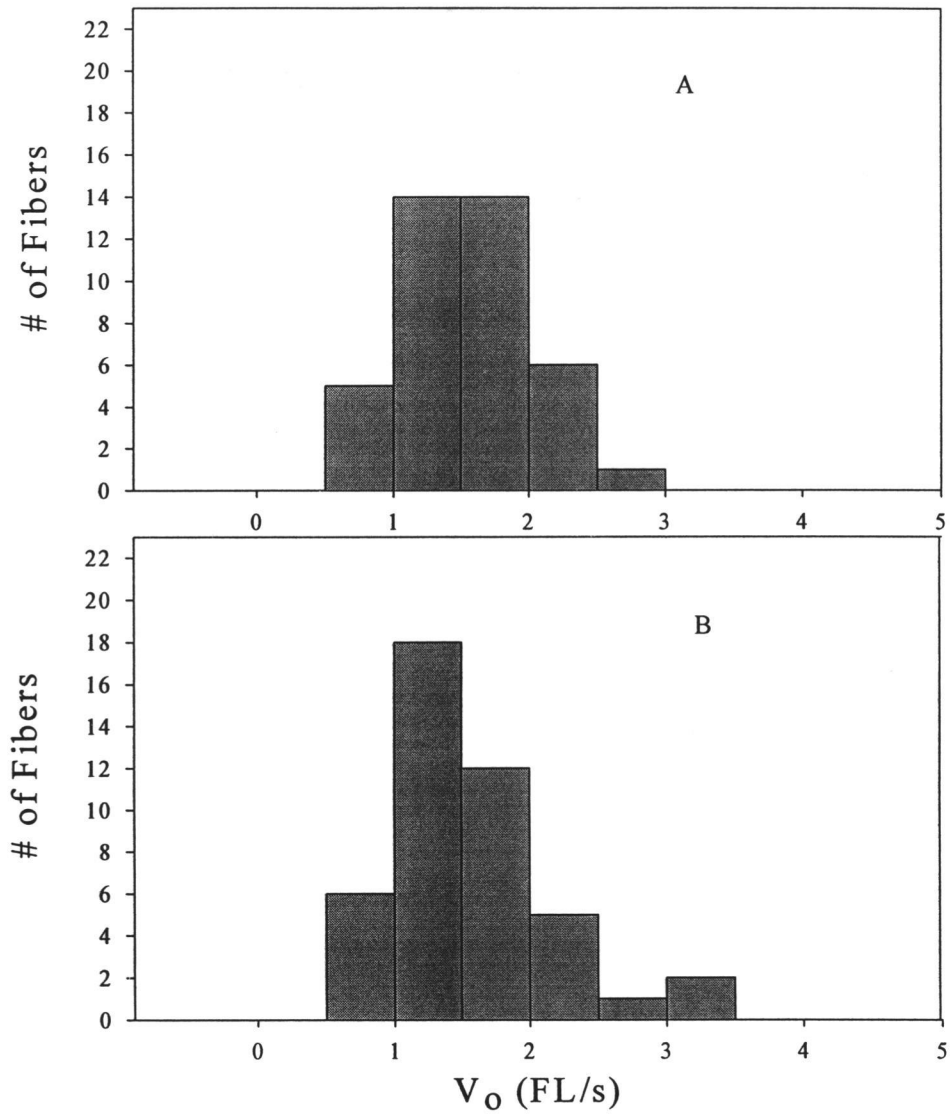
Figure 3.1 Histograms of V_o for type I fibers from C57BL/6 mice. Histograms depicts the shortening velocity distribution of type I fibers before (panel A) and following hindlimb suspension (panel B).

chose to study the soleus for two reasons. First, according to rat and human studies, the soleus is the muscle most affected by non-weight bearing (Fitts et al., 2000; Gardetto et al., 1989; Widrick et al., 1999). Second, the soleus appears to be the only hindlimb muscle of the mouse that has an appreciable population of slow fibers (Carlson et al., 1999; Warren et al., 1994; Marechal and Beckers-Bleukx, 1993). Finally, the soleus muscle, because of its distinct proximal and distal tendons and small size, it is amenable for in situ or in vitro preparations (Ingalls et al., 2001; Ingalls et al., 1999; Haida et al., 1989; Warren et al., 1994). Thus, an understanding of the changes occurring in the cells comprising this muscle is necessary for the interpretation of data obtained at the intact muscle level.

In terms of gross soleus atrophy, our findings are similar to other studies of HS with mice. Previous mouse 7-day HS studies have reported 25-42% reductions in soleus mass (Steffen et al., 1984; Criswell et al., 1998a; Ingalls et al., 2001; Carlson et al., 1999) and 16-59% reductions in soleus mass/body mass ratio (Criswell et al., 1998a; Carlson et al., 1999). Thus, despite having a 2-fold higher resting metabolic rate (Taylor et al., 1970) and a substantially different MHC profile, the time course and the amount of gross atrophy in the mouse soleus muscle are similar to the rat. Atrophy of other hindlimb muscles in this study are also similar to previous studies of HS with mice (McCarthy et al., 1997; Carlson et al., 1999; Criswell et al., 1998b; Steffen et al., 1984), showing that significant atrophy occurs following HS in the gastrocnemius, plantaris, and tibialis anterior, while the extensor digitorum longus is unaffected.

The low distribution (20%) of type I fibers in the C57BL/6 soleus makes it essentially a fast muscle. Other mouse strains have been reported to have soleus type I fiber composition that ranges from 35-75% (Haida et al., 1989; Wernig et al., 1990). We chose to study the C57BL/6 strain because it is the most commonly used inbred strain (Maher, 2002) in biomedical research making up 14% of all of studies using inbred strains (Festing, 2002).

Based on ATPase histochemistry some investigators (McCarthy et al., 1997) have reported that the distribution of slow fibers in the mouse soleus decreases during HS while others have reported the opposite (Haida et al., 1989). It has been suggested (McCarthy et al., 1997) that the discrepancy in the literature may have been due to differences in the acid preincubation conditions used for the analysis of ATPase activity. The present data, where we used SDS-PAGE to evaluate the MHC isoform content of soleus homogenates, revealed that the distribution of type I, IIa, and IIb isoforms was not altered by 7 days of HS. Analysis of muscle homogenates provides no information on how MHC isoforms are distributed within fibers, which is the physiologically relevant parameter. Analysis of fibers may also reveal information on transitions between isoforms. Therefore, in addition to the fibers used in the functional analysis, we also analyzed approximately 1000 additional soleus fibers for MHC content. The results of this analysis were consistent with the whole muscle analysis in that 7 days of HS had little effect on MHC distribution.

The mouse strain (FVB/n) used by McCarthy et al. (1997) had a high percentage of type I soleus fibers (percent not reported but histochemical analysis revealed high density of type I fibers) whereas the strain (129B6F$_1$/J) used by Haida et al. (1989) and in the present study had low percentages of type I soleus fibers (35% and 20%, respectively). Therefore, we propose that relative distribution of type I fibers in the mouse soleus may determine the response of the muscle to HS. Solei with high expression of type I MHC show a reduction in this isoform with HS. Solei that contain relatively low levels of slow MHC show no change in isoform distribution with HS. The FVB/n strain falls into the first category and the 129B6F$_1$/J and C57BL/6 strains fall into the second. Our proposal is consistent with studies of non-weight bearing in rats (Ohira et al., 1992; Caiozzo et al., 1994; Talmadge et al., 1996), and humans (Widrick et al., 1999; Edgerton et al., 1995), showing that the population of type I fibers decreases and the population type II fibers increases. Thus, we propose that changes in MHC isoform distribution with HS are more variable in the mouse because of the large variability in the MHC composition of the soleus across strains.

In the present study HS caused a decrease in CSA of both type I and IIa fibers (33%). These changes are similar to those reported by Haida et al. (1989) who found that after 2 weeks of HS, type I fibers atrophied 37% and type II fibers atrophied 46%. Edgerton and Roy (1996) reported that in humans and rats the greater the fiber diameter before non-weight bearing, the greater the atrophy following non-weight bearing. This hypothesis appears to hold true for rats and

humans because in rats type I fibers have a greater CSA than type IIa fibers, while the reverse is true in humans (Widrick et al., 1999). The results of this study are in general agreement with this notion since type I and IIa fibers were of similar CSA and experienced a similar degree of atrophy.

We observed a substantial decrease in the absolute Ca^{2+}-activated force (mN) of single fibers expressing type I MHC (46%) and type IIa MHC (47%) with 7 days of HS. These differences persisted when values were normalized for fiber CSA, as the specific force of fibers declined 17%, and 20% in fibers expressing type I and IIa MHC, respectively. This indicates that in addition to a loss in fiber CSA, the intrinsic ability of the fibers to produce force declined. The mechanisms responsible for the decline in specific force cannot be due to excitation-contraction failure since the fibers are activated with a saturating amount of Ca^{2+}. Instead, the specific force decrements following non-weight bearing are likely due to a disproportionate loss of myofibrils which would decrease the number of strongly bound cross-bridges per unit of fiber volume (Fitts et al., 2000). Studies of non-weight bearing with rats (Widrick et al., 1996; Gardetto et al., 1989) and humans (Widrick et al., 1999) show that normalized force (kN/m^2) decreases in type I fibers but not in type IIa fibers. It is clear that in the C57BL/6 mouse, both the absolute and the specific force of fibers expressing IIa MHC are as affected as fibers expressing type I MHC.

In the present study the V_o of fibers expressing type I MHC was unaltered by 7 days of HS. This is in contrast to the majority of studies of non-weight bearing

in rats (Widrick et al., 1996; McDonald et al., 1994; Gardetto et al., 1989) and humans (Widrick et al., 1999), which show that the V_o of soleus fibers expressing type I MHC rises. The increase in type I fiber V_o in rats and humans has been hypothesized to be a protective response to attenuate or reduce the loss of power despite decreased force (McDonald et al., 1994; Caiozzo et al., 1996). Since there is a drop in P_o but no corresponding rise in shortening velocity, we predict that power will decline relatively more in atrophied slow fibers of the C57BL/6 soleus than in rat or human fibers.

Quiet standing activity in bipeds requires near maximal soleus recruitment (Walmsley et al., 1978). Thus, in the predominately slow soleus of the rat, virtually all of the type I fibers would be recruited during normal weight bearing activity. The situation for the C57BL/6 mouse would be quite different where weight bearing activity would necessitate activation of much of the type II fiber population in addition to the type I motor units. If this hypothesis of fiber recruitment is accurate, then removal of weight bearing activity will greatly reduce the tonic, externally loaded contractile activity experienced by both type I and type II fibers in the C57BL/6 soleus. Finally, if the absence of tonic externally loaded contractile activity is a primary cause of soleus muscle fiber atrophy, one would predict roughly similar atrophy of type I and II fibers in the C57BL/6 soleus. This prediction is consistent with the results reported here.

Note that this model is based on motor unit recruitment rather than on MHC isoform expression. Previous studies examining rats and humans, species with

predominately slow soleus muscles, have suggested that type I fibers are more sensitive to non-weight bearing atrophy than type II fibers. This conclusion was reached by comparing either slow and fast fibers from anatomically different muscles, or slow and fast fibers obtained from a phasic muscle. A novel aspect of the present study is that we examined an animal with a mixed soleus muscle MHC isoform profile and were thus able to study substantial numbers of slow and fast fibers from the same postural muscle. Our results suggest that a model to explain fiber susceptibility to atrophy that is based on motor unit recruitment is more generalizable than a model based on fiber MHC isoform expression. It is important to note that our data were obtained from the tonic soleus and the model may not be applicable to phasic muscles, such as the gastrocnemius.

An advantage of the mouse model for non-weight bearing study is that it has a type I fiber soleus population has been reported to range between 20% (present study) and 75% (Wernig et al., 1990) depending on the strain. Therefore, it may be possible to study the effects of non-weight bearing on single fibers expressing type I and IIa MHC from a predominantly fast soleus muscle (C57BL/6 mouse) or a predominantly slow one (CBA/J mouse). The ability to create transgenic mouse models provides a unique opportunity to study and understand the regulatory mechanisms and genes that govern response to HS in an intact animal (Tsika, 1994).

The main disadvantage to the use of the mouse model is that its muscles, and especially the soleus, are much smaller the rat. There is consequently, less

tissue available for biochemical, histological, and molecular studies. Similarly, mouse skinned fibers are substantially smaller in CSA than fibers from the rat, especially after HS. While this makes their study technically more difficult, the present study demonstrates the feasibility of studying single fibers from mice after 7 days of HS.

The present study indicates that 7 days of HS produced significant atrophy and decreases in force per CSA in type I and type IIa fibers from the C57BL/6 mouse soleus. Maximal shortening velocity of type I and IIa fibers was unaltered by HS. The changes that occur with non-weight bearing in the C57BL/6 mouse soleus appear to be similar to the changes occurring in rat and human solei with respect to general trends of fiber atrophy and decreases in force per CSA. However, in contrast to those other species, the mouse type I and IIa fibers are equally affected in terms of fiber atrophy and reductions in absolute and specific force. Furthermore, the changes observed in this study regarding changes in fiber V_o are different than the rat or human models, especially in type I fibers. These findings suggest that at least in some aspects, the mouse model of HS is different than the rat model. However, these results need to be interpreted with caution since unlike the rat soleus the C57BL/6 mouse soleus expresses a majority of fast type IIa fibers. The question still remains whether the response of the C57BL/6 mouse to HS is due to characteristics of strain or species. To further elucidate the response of the mouse model to non-weight bearing, other strains of mice containing more similar soleus muscle compositions to the rat may need to be studied.

Chapter 4

Functional Responses of Soleus Muscle Fibers from ICR and CBA/J Mice
to 7 Days of Hindlimb Suspension

Julian E. Stelzer and Jeffrey J. Widrick

Department of Exercise and Sport Science

Abstract

Hindlimb suspension (HS) increases maximal shortening velocity (V_o) of type I fibers from the rat soleus, a predominantly slow (90% type I fibers) muscle. We recently reported that 7 days HS did not change the V_o of type I fibers from the soleus of C57BL/6 mice, a predominantly fast (80% type IIa fibers) muscle. The purpose of this study was to test the hypothesis that mice with greater soleus type I myosin heavy chain (MHC) expression would show HS-induced changes in type I fiber V_o comparable to those of the rat. Skinned muscle fibers were prepared from solei of 7 day HS and weight-bearing (WB) ICR and CBA/J mice (50% type I MHC composition) and studied using an in vitro single cell preparation. HS increased the amount of type IIa MHC present in the soleus and caused significant fiber atrophy, decreases in specific peak Ca^{2+}-activated force of type I and IIa fibers, and increases of type I fiber V_o for both strains of mice. These changes in soleus MHC isoform expression, fiber peak force, and fiber V_o are similar to those changes observed in the rat HS model.

Introduction

Hindlimb suspension (HS) causes a shift in the myosin heavy chain (MHC) profile of the rat soleus muscle from predominantly slow MHC to a mixed expression of slow and fast isoforms (Caiozzo et al., 1998; Caiozzo et al., 1997; Thomason and Booth, 1990; Edgerton and Roy, 1996). Additionally, the maximal shortening velocity (V_o) of rat soleus type I fibers has been reported to be elevated following HS (Widrick et al., 1996; McDonald et al., 1994; Gardetto et al, 1989; Bangart et al., 1997; Reiser et al., 1987; Thompson et al., 1998). The shift in soleus MHC composition and the increase of type I fiber V_o following HS may attenuate or decrease the muscle power deficits associated with fiber atrophy and muscle fiber force (McDonald et al., 1994; Fitts et al., 2000).

Recently, our laboratory studied the effects of 7 days of HS on the contractile function of skinned muscle fibers from the C57BL/6 mouse soleus (Stelzer and Widrick, 2002). The C57BL/6 mouse is the most commonly used strain in biomedical research (Maher, 2002). The C57BL/6 mouse responded in a similar way as other species that experienced non-weight bearing with respect to whole muscle and single fiber atrophy, and decreases of single fiber absolute and specific force, but interestingly, there was no change in soleus MHC isoform content or in single fiber V_o. A possible explanation for the lack of change in V_o following HS in this particular strain may be due to its unusual soleus muscle composition. This muscle contains only 20% type I MHC, making it essentially a

fast muscle that is much different in MHC composition and function from the 85-90% slow type I MHC rat soleus (Delp and Duan, 1996; Thompson et al., 1998). This finding raised questions regarding the efficacy of the mouse model for the study of skeletal muscle responses to non-weight bearing at the single fiber level.

Since we are aware of no data on mouse single fiber contractile function following HS, it was not possible to determine whether our data reflected a species difference between rats and mice in response to HS, or alternatively, that the in-bred C57BL/6 strain, with its uncharacteristically fast soleus, responded differently to non-weight bearing. The mouse has potential to replace the rat as the species of choice in studies of non-weight bearing and muscle function because its smaller maintenance cost and size makes it ideal for use in environments where room and resources are limited, such as aboard the Space Shuttle or the International Space Station. More importantly, the availability of genetically modified mice will likely play key roles in developing and testing hypotheses related to protein-function relationships. However, if the mouse is to replace the rat as the primary model of non-weight bearing, it is necessary to establish the similarities and differences between the two species in response to non-weight bearing.

The purpose of this study was to evaluate the effects of 7 days of HS on soleus MHC composition and single fiber contractile function of ICR and CBA/J mice. These strains were chosen because their solei have been reported to contain at least 50% type I MHC, and because they represent an out-bred and an in-bred strain, respectively. Our study elucidates the role muscle MHC composition plays

on single fiber contraction function following HS, and establishes whether the

mouse model is a suitable alternative to the rat model of non-weight bearing.

Methods

<u>Animal care and suspension procedure</u>

All protocols were approved by the Oregon State University Institutional

Animal Care and Use Committee (IACUC). Male ICR (also designated as CD-1)

and CBA/J mice (25-30 grams) were obtained from Harlan Laboratories,

acclimated for a 7-day period at Oregon State University Animal Care Facility, and

then randomly assigned to the hindlimb suspension (HS) (ICR: n=5, CBA/J: n=5)

or weight bearing groups (WB) (ICR: n=6, CBA/J: n=6). Both groups were

maintained on a similar diet of laboratory chow (ad libitum) and water. Animals

were housed at 23°C with a 12:12 hour light-dark cycle.

The hindlimb suspension protocol was identical to that used in our earlier

study on C57BL/6 mice (Stelzer and Widrick, 2002). Briefly, mice were suspended

by their tails for 7 days using a tail harness. Strips of adhesive tape were glued in a

helical pattern to the base of the tail and extended to approximately two-thirds of

the tail's length with cyanoacrylate glue. Next, a triangle shaped 18-gauge wire was

secured to the base layer of tape with additional strips of adhesive tape. The

triangle shaped wire was positioned so its apex pointed upward, where a fishing

line swivel was clipped to the wire. Monofilament line was fastened to the swivel

and passed through a small hole in a sheet of Plexiglas that served as the 'ceiling' of the suspension apparatus. The length of the monofilament line was raised such that the hindlimbs of the animals were elevated off the grid floor and were not touching supportive surfaces. The forelimbs remained in contact with a grid floor, which allowed the animals to move about in a 360° circle and feed and drink (ad libitum). Waste passed through the grid onto absorbent paper. The exposed tip of the tail was monitored daily to ensure adequate blood flow.

Surgical procedures

Mice were anesthetized with an intraperitoneal injection of pentobarbital sodium (40 mg/kg body mass). In order to prevent any reloading-induced muscle damage, non-weight bearing mice were anaesthetized while still suspended. When mice were lowered their tale harness was removed and they were immediately weighed. The left soleus was excised, weighed, and immediately prepared for use in skinned single fibers experiments (see below). The right hindlimb muscles, including the soleus, plantaris, gastrocnemius, tibialis anterior, and extensor digitorum longus, were removed, trimmed of connective tissue and fat, weighed, and frozen in liquid nitrogen. The soleus muscle samples were stored at -80°C, and later used for the determination of whole muscle myosin heavy chain (MHC) isoform distribution.

Tissue preparation

The left soleus muscle was placed in relaxing solution (for composition, see below) and dissected into 2-3 longitudinal bundles. The muscle bundles were placed in a skinning solution, consisting of 50% dissection solution and 50% glycerol (for composition see below). This solution disrupts membranes and organelles, including the sarcolemma, and the sarcoplasmic reticulum. Bundles were refrigerated at 4°C for 24 hours and then placed in fresh skinning solution and stored at -20°C for up to 4 weeks.

Solutions

The composition of solutions used for single fiber experiments were derived from the computer program described by Fabiato (1988). Stability constants used in these calculations were adjusted for the experimental conditions of this project (Fabiato, 1985). Relaxing and activating solutions contained: 4 mM Mg^{2+}-ATP, 1 mM of free Mg^{2+}, 20.0 mM imidazole, 7.0 mM EGTA, 14.5 mM creatine phosphate, 15 $U \cdot ml^{-1}$ creatine kinase, and sufficient KCl and KOH to adjust the ionic strength to 180 mM and the pH to 7.0, respectively. The relaxing and activating solutions contained a total free Ca^{2+} concentration of pCa 9.0 and pCa 4.5, respectively (where pCa = -log $[Ca^{2+}]$), which was adjusted with $CaCl_2$ (Calcium Molarity Standard, Corning Inc., Corning, NY).

The dissection solution was composed of relaxing solution mixed with a cocktail of protease inhibitors prepared to manufacturer specifications (Complete

Mini EDTA-Free Protease Inhibitor tablets, Boehringer Mannheim, Indianapolis, IN). The skinning solution contained equal volumes of dissection solution and glycerol.

Single fiber experiments

Single fibers were isolated from muscle bundles while immersed in cold relaxing solution. The ends of an isolated single fiber were mounted to stainless steel troughs which were connected to a direct-current position motor (Model 308B, Aurora Scientific, Ontario) and an isometric force transducer (Model 400, Aurora Scientific) using 4-0 monofilament posts and 10-0 suture (Widrick, 2002). The fiber was suspended in one of three chambers milled into a stainless steel plate. The plate was mounted on an inverted microscope (Olympus IX-70, Olympus America Inc., Melville, NY) making it possible to view the fiber at 600X through the transparent bottom of each chamber. Sarcomere length was adjusted to 2.5 μm using a calibrated ocular micrometer and 3-axis micromanipulators mounted to the motor and force transducer. Fiber length (FL) was determined using a digital micrometer mounted to the mechanical stage of the microscope. Fiber cross-sectional area (CSA) was calculated while the fiber was suspended in air by measuring the diameter at three points along the length of the fiber under the assumption that the fiber forms a cylinder in air (Metzger and Moss, 1987; Widrick, 2002). The average of the 3 measurements was taken as the fiber CSA.

All experiments were performed at 15°C and temperature was continuously monitored with a thermocouple inserted into the experimental chamber.

Force and position outputs were viewed on a digital oscilloscope (Model Integra 10, Nicolet Technologies, Madison, WI). The signals were amplified, digitized (5 kHz), and interfaced to a personal computer by a data acquisition board (Model AT-MIO-16E, National Instruments, Austin, TX). Data acquisition, storage, and analysis were controlled through a custom computer program (written in LabView, National Instruments, Austin, TX).

Depressing the stainless steel plates allowed the transfer of fibers from the chamber containing relaxing solution to the chamber containing activating solution. Unloaded shortening velocity (V_0) and peak Ca^{2+}-activated force (P_0) were determined using the slack test method (Edman, 1979). In this procedure, a series of slack steps ($\leq 20\%$ of FL) were applied to the fiber and the time to force re-development was measured. A minimum of five different slack step lengths were plotted versus the corresponding times required for tension re-development. The plot was fit by a least squares linear regression. The slope of the regression line normalized to fiber length was defined as V_0. Peak Ca^{2+}-activated force was determined as the difference between the maximum force preceding the slack step and the force baseline acquired during unloaded shortening. Specific force was calculated by dividing peak isometric force by fiber CSA.

Gel electrophoresis

After contractile analysis, the fiber was solubilzed in 30 µl of SDS sample buffer (containing 10% glycerol, 5% beta-mercaptoethanol, 2% SDS, 62.5 mM Tris (pH 6.8), and 0.001% bromophenol blue), denatured for 4 minutes at 95°C, and stored at -80°C. Fiber myosin heavy chain (MHC) content was determined by taking a 2 µl sample of the fiber solute and running it on a discontinuous polyacrylamide gel system consisting of a 7% separating gel and a 3.5% stacking gel (Fauteck and Kandarian, 1995). Electrophoresis was carried out on a Bio-rad mini-Protean 3 electrophoresis system (Bio-Rad Laboratories, Hercules, CA) running at 70 V for 24 hours (4°C). Myosin heavy-chain content of soleus whole muscles was determined by extracting myosin from samples of mouse soleus (LaFramboise et al., 1990) and running samples on similar gels. A silver staining procedure (Shevchenko et al., 1996) was used to visualize protein bands.

Densitometry

Relative hybrid composition was assessed using laser-scanning densitomery (Molecular Dynamics, ImageQuaNT 5.0, Sunnyvale, CA). Gels were scanned for 100-micron pixel size and area integration was performed to determine relative density of each MHC band present in muscle samples or in fibers containing multiple MHC isoforms.

<u>Statistical analysis</u>

Mean values for WB and HS groups for each mouse strain were analyzed with a two-way analysis of variance with treatment and mouse strain as the main effects. A Tukey post-hoc test was run on statistically significant differences. Statistical significance was accepted as $p < 0.05$. All statistics were performed using SPSS version 10.0 (SPSS Inc., Chicago, IL).

Results

<u>Body and hindlimb muscle mass changes with HS</u>

Seven days of HS decreased the body mass of ICR mice (WB: 28.8 ± 1.1 grams, HS: 24.3 ± 1.6 grams, $p < 0.05$) and CBA/J mice (WB: 26.6 ± 0.7 grams, HS: 22.3 ± 0.9 grams, $p < 0.05$). The change was similar for both strains (16%). Significant strain effects indicated that absolute muscle mass and muscle mass relative to body mass were greater for gastrocnemius, plantaris, and extensor digitorum longus of CBA/J mice prior to HS (Table 4.1). Seven days of HS caused muscle atrophy of the soleus, plantaris, gastrocnemius, and tibialis anterior, for both ICR and CBA/J mice. Atrophy of the plantaris and gastrocnemius occurred in proportion to the loss in body mass since there was no significant treatment effect for muscle mass/BM for either muscle. Atrophy of the tibialis anterior was related to the loss of body mass because muscle mass/BM was not affected by HS. There was no change in absolute mass of the extensor digitorum longus in either strain.

Table 4.1. Effect of 7 days of HS on hindlimb muscle mass
of ICR and CBA/J mice

Muscle	Strain	Treatment	Muscle Mass (mg)	Muscle mass/BM
SOL	ICR	WB	7.4 ± 0.3	0.257 ± 0.009
		HS	4.2 ± 0.4*	0.171 ± 0.008*
	CBA/J	WB	6.8 ± 0.4	0.255 ± 0.014
		HS	5.3 ± 0.4*	0.237 ± 0.017
PLT	ICR	WB	14.6 ± 1.2	0.508 ± 0.036
		HS	11.5 ± 0.7	0.479 ± 0.030
	CBA/J	WB	17.3 ± 0.6	0.651 ± 0.022
		HS	14.6 ± 0.5	0.657 ± 0.014
GAST	ICR	WB	118.2 ± 7.9	4.089 ± 0.157
		HS	85.8 ± 2.1	3.588 ± 0.227
	CBA/J	WB	131.9 ± 3.6	4.961 ± 0.090
		HS	112.4 ± 3.6	5.044 ± 0.139
TA	ICR	WB	47.0 ± 2.4	1.633 ± 0.057
		HS	36.2 ± 1.1	1.506 ± 0.067
	CBA/J	WB	43.8 ± 0.9	1.650 ± 0.050
		HS	38.5 ± 1.4	1.725 ± 0.046
EDL	ICR	WB	9.3 ± 0.5	0.324 ± 0.018
		HS	7.4 ± 0.3	0.309 ± 0.012
	CBA/J	WB	13.0 ± 0.5[†]	0.490 ± 0.013
		HS	12.9 ± 0.5	0.581 ± 0.020*

Values are mean ± SE of 5-6 muscles. Abbreviations: WB, weight bearing; HS, hindlimb suspended; SOL, soleus; PLT, plantaris; GAST, gastrocnemius; TA, tibialis anterior; EDL, extensor digitorum longus; muscle mass/BM, muscle mass/body mass. Asterisk denotes significant difference from corresponding WB muscle ($p < 0.05$), [†] denotes significant strain effect for muscle mass and muscle mass/BM ($p < 0.05$).

However, there was a significant interaction in mass/BM due to an increase in value for CBA/J. This was related to the fact that despite loss in body mass, the mass for the extensor digitorum longus from this strain was essentially the same mass after HS as before.

Muscle MHC content

Soleus muscles from WB ICR and CBA/ mice both contained 49% type I MHC, with the remainder being type IIa MHC (Table 4.2). Solei from HS ICR and CBA/J mice had a significant decrease in soleus muscle type I MHC after 7 days of HS. This decrease averaged 17% and 14%, for ICR and CBA/J mice, respectively, with a corresponding increase in soleus type IIa composition (Table 4.2).

Fiber cross-sectional area and peak Ca^{2+}-activated force

A total of 392 fibers were included in the contractile function analysis: 209 from the WB (ICR; n=91; CBA/J: n=116) animals and 183 from 7-day HS (ICR: n=90; CBA/J: n=93) animals. All fibers isolated for analysis expressed type I or type IIa MHC isoform.

Fiber cross-sectional area (CSA), peak Ca^{2+}-activated force (P_o), and specific force (P_o /CSA) data are presented in Table 4.3. When directly activated with Ca^{2+}, peak force was 47% lower in type I fibers obtained from HS ICR mice. This was a result of type I fiber atrophy (39%) coupled with a reduction in fiber force per cross-sectional area, or specific force (13%). The type IIa fibers from ICR

Table 4.2. Effect of 7 days of HS on soleus MHC isoform distribution
of ICR and CBA/J mice

		Percent Distribution			
Strain	Group	MHC I	MHC IIa	MHC IIx	MHC IIb
ICR	WB	49.2 ± 2.4	50.8 ± 2.4	nd	nd
	HS	32.0 ± 3.1*	68.0 ± 3.1*	nd	nd
CBA/J	WB	49.0 ± 0.6	51.0 ± 0.6	nd	nd
	HS	34.6 ± 2.9*	65.4 ± 2.9*	nd	nd

Values are mean ± SE of 5-6 muscles. Soleus muscle percent distribution
determined by densitometry. Abbreviations: WB, weight bearing; HS, hindlimb
suspended; MHC, myosin heavy chain; nd, not detected. Asterisk denotes
significant difference from corresponding WB value (p<0.05).

Table 4.3. Effect of 7 days of HS on CSA, P_o, and P_o/CSA of type I and IIa soleus fibers of ICR and CBA/J mice

MHC	Strain	Treatment	n	CSA (μm^2)	P_o (mN)	P_o/CSA (kN/m^2)
I	ICR	WB	48	1500 ± 45	0.18 ± 0.01	117 ± 1
		HS	40	916 ± 33*	0.09 ± 0.01*	102 ± 1*
	CBA/J	WB	44	1380 ± 39	0.16 ± 0.01	117 ± 2
		HS	43	910 ± 30*	0.10 ± 0.01*	104 ± 2*
IIa	ICR	WB	43	1049 ± 34	0.12 ± 0.01	116 ± 1
		HS	50	828 ± 37*	0.09 ± 0.01*	101 ± 1*
	CBA/J	WB	72	$1408 \pm 37^\dagger$	$0.16 \pm 0.01^\dagger$	114 ± 1
		HS	50	922 ± 29*	0.11 ± 0.01*	100 ± 1*

Values are mean ± SE. Abbreviations: MHC, myosin heavy chain; WB, weight bearing; HS, hindlimb suspended; n, number of fibers isolated from muscle bundles; CSA, cross-sectional area; P_o, peak isometric force; P_o/CSA; peak isometric force per cross-sectional area. Asterisk denotes significant difference from WB (p<0.05), † denotes significant difference from ICR strain (p<0.05).

mice showed significant reductions in CSA (21%), peak Ca^{2+}-activated force (31%), and specific force (13%) following HS. The response of the CBA/J mouse fibers to HS was similar to that observed for the ICR mouse fibers. Peak Ca^{2+}-activated force of CBA/J type I fibers was 41% lower following HS due to fiber atrophy (34%) and a reduction in fiber specific force (11%). Type IIa fibers from CBA/J mice were larger in CSA (25%) and produced more force (25%) than type IIa fibers from ICR mice prior to HS. Type IIa fibers from CBA/J mice experienced 35% atrophy, a 34% decrease in peak Ca^{2+}-activated force, and an 11% decrease in specific force.
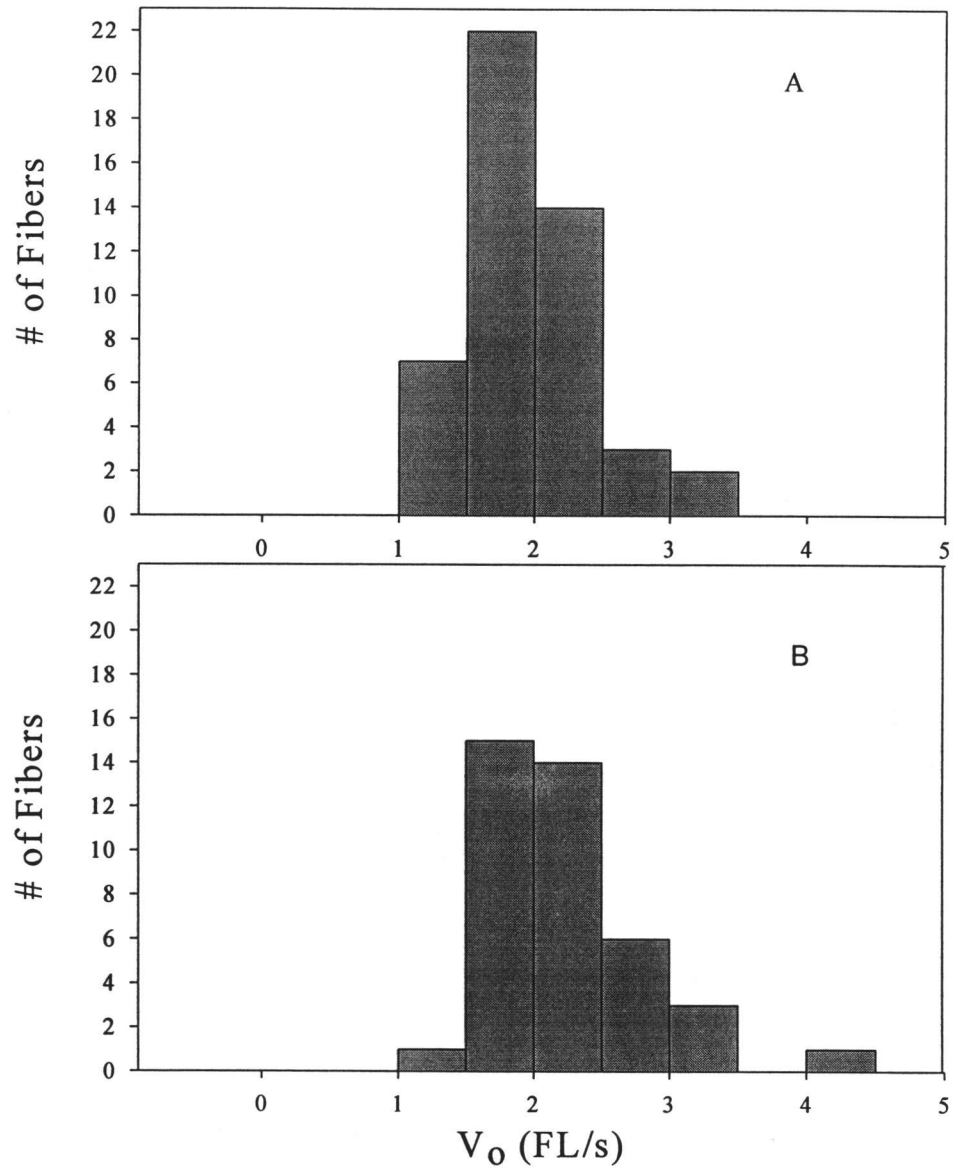
<u>Unloaded shortening velocity</u>

Type I V_0 increased significantly for both strains (ICR: 14%; CBA/J: 16%) following HS (Table 4.4). Type IIa fibers from ICR mice showed a trend towards increased V_0 following HS, but the change was not statistically significant (p=0.10).

Maximal shortening velocity-frequency distribution histograms before and after HS for type I fibers from ICR (Figure 4.1) and CBA/J (Figure 4.2) mice show that there was an increase in the number of fibers with high V_0 and a decrease in the number of fibers with low V_0 following HS. Maximal shortening velocity-frequency distribution histograms for the pre-HS ICR type IIa fibers suggested a bimodal distribution with modes at approximately 2.5-3.0 FL/s and at 4.5-5.0 FL/s (Figure 4.3).

Table 4.4. Effect of 7 days of HS on V_o on type I and IIa soleus fibers
of ICR and CBA/J mice

MHC	Strain	Treatment	V_o (FL/s)
I	ICR	WB	1.95 ± 0.07
		HS	2.22 ± 0.10*
	CBA/J	WB	1.93 ± 0.09
		HS	2.24 ± 0.12*
IIa	ICR	WB	3.45 ± 0.14
		HS	3.96 ± 0.18
	CBA/J	WB	3.65 ± 0.12
		HS	3.51 ± 0.14

Values are mean $\pm$ SE. Number of fibers is the same as Table 4.3. Abbreviations: MHC, myosin heavy chain; WB, weight bearing; HS, hindlimb suspended; V_o, maximal shortening velocity; FL/s, fiber lengths per second. Asterisk denotes significant difference from WB ($p < 0.05$).

Figure 4.1 Histograms of V_o for type I fibers from ICR mice. Histograms depicts the shortening velocity distribution of type I fibers without (panel A) and with HS (panel B) for ICR mice.
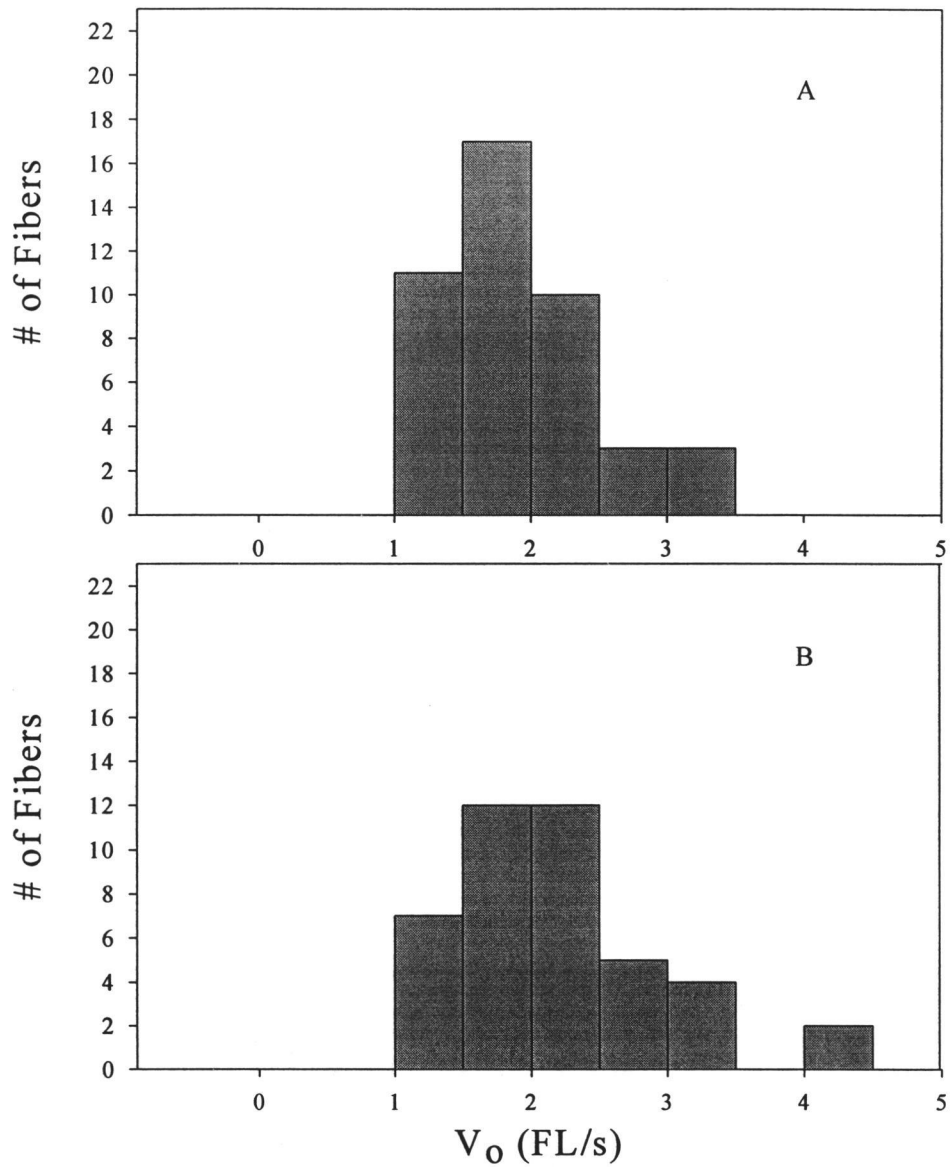
Figure 4.2 Histograms of V_o for type I fibers from CBA/J mice. Histograms depicts the shortening velocity distribution of type I fibers without (panel A) and with HS (panel B) for CBA/J mice.
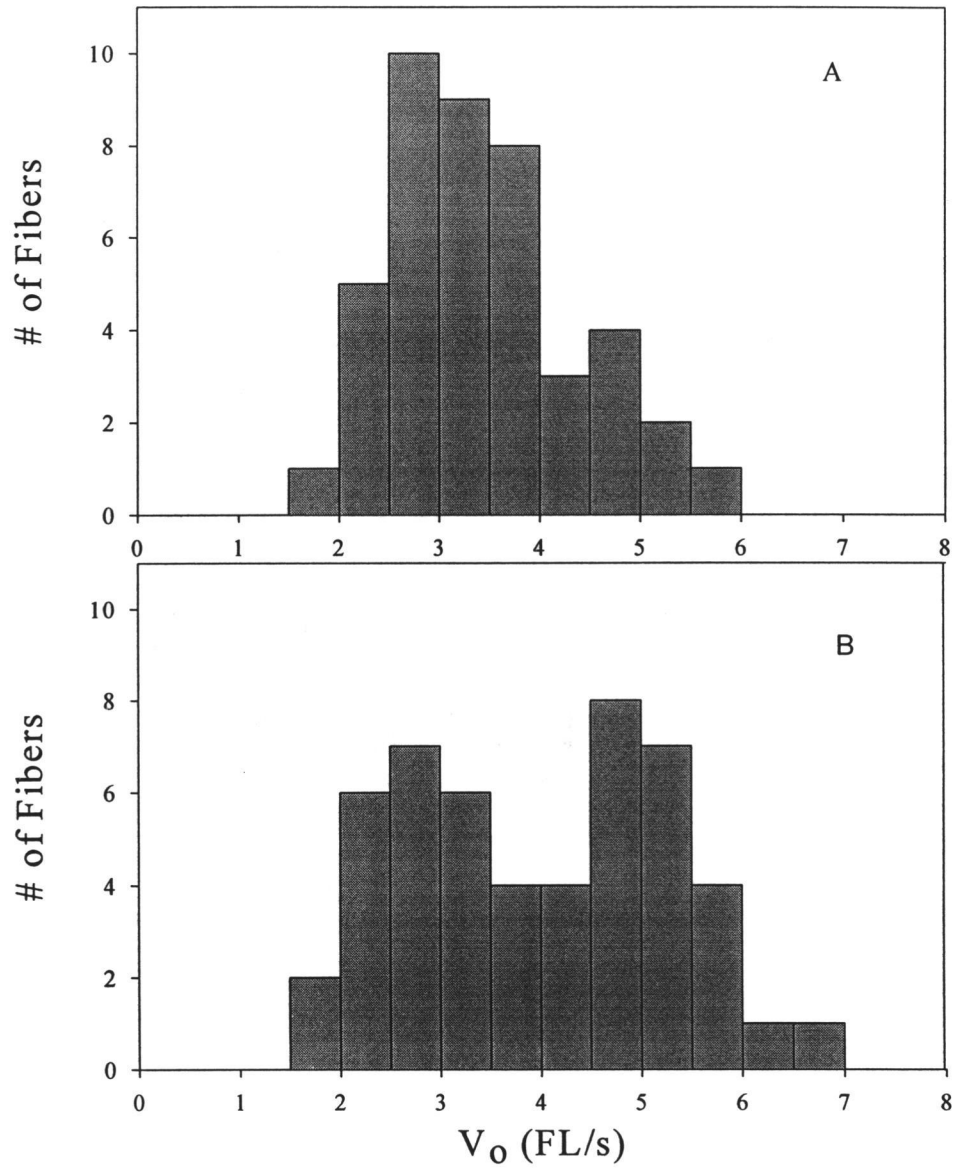
Figure 4.3 Histograms of V_o for type IIa fibers from ICR mice. Histograms depicts the shortening velocity distribution of type IIa fibers without (panel A) and with HS (panel B) for ICR mice.

After HS, there appeared to be a decrease in the proportion of fibers at the lower mode and an increase in fibers at the higher mode.

Discussion

Our aim was to examine the effects of 7 days of HS on the contractile function of skinned single fibers from mouse strains containing a soleus muscle fiber composition that is more similar to the rat and human. Our findings indicate that mouse strains with a soleus MHC composition more similar to the rat respond to HS in a similar manner as the rat model of HS. However, whether this response is due exclusively to the difference in MHC isoform content, or to other unidentified differences between strains, is not known.

The soleus muscle atrophy experienced by both strains of mouse in the present study is consistent with findings of other studies of HS with mice including our own previous study on C57BL/6 mice (Steffen et al., 1984; Carlson et al., 1999; Ingalls et al., 2001; Criswell et al., 1998a). Despite having identical soleus muscle fiber composition, the ICR strain experienced a two-fold greater atrophy of the soleus muscle compared to the CBA/J strain. These observations indicate that there is large variability in soleus muscle atrophy following HS between the ICR and CBA/J strains. The non-significant decrease in soleus mass to body mass ratio in the CBA/J strain was an indication of the large variability of body mass decreases experienced by individual mice following HS and not the variability of

soleus atrophy as indicated by the significant atrophy at the single fiber level experienced by all CBA/J mice (Table 4.3). These differences may reflect the behavioral response of different strains to the HS model. Liu and Gershenfeld (2001) reported that the behavioral responses and activity levels of HS mice varied dramatically across strains. Subjectively, the C57BL/6 and CBA/J strains appeared to be more aggressive and active than the ICR mice. Thus, the strain that appeared the least active experienced the most atrophy.

Examination of whole muscle weights in the three different strains of mouse reveals that despite having similar body mass, there was variability in the mass of the soleus muscle. The C57BL/6 strain had the smallest body mass yet its soleus mass was 27% and 20% greater than the ICR and CBA/J strains, respectively. Furthermore, the ICR and CBA/J strains' soleus muscles were composed of an equal amount of slow type I and fast type IIa fibers while the C57BL/6 soleus is composed of 20% type I MHC, 77% IIa, and 3% IIb fibers. However, the relative importance of these variables remains unclear since despite having vastly different soleus muscle MHC composition, the C57BL/6 and CBA/J strains experienced similar relative atrophy following HS.

Previous studies of HS with mice have reported conflicting results with respect to shifts in fiber type composition (McCarthy et al., 1997; Haida et al., 1989). McCarthy et al. (1997) reported that the relative number of type I fibers decreased in the predominantly slow soleus muscle from the FVB/n mouse. Conversely, Haida et al. (1989) reported that the relative number of type I fibers

increased in the predominantly fast soleus muscle from the 129B6F$_1$/J mouse. Results from our previous study (Stelzer and Widrick, 2002) revealed no shift in the MHC composition of the predominantly fast (~80% type IIa MHC) soleus muscle from the C57BL/6 strain following HS.

The 14-17% decrease in soleus type I MHC composition, with a corresponding increase in type IIa MHC composition, observed for both strains in the present study, are consistent with McCarthy et al. (1997). Not surprisingly, the mouse strains used in the latter and the present study have soleus muscles that are composed of at least 50% type I MHC. Taken together, these data suggest that soleus MHC composition shifts that occur in the mouse soleus following HS may be dependent on the soleus MHC composition of the particular strain. Mice strains that contain a high amount of soleus slow type I MHC (at least 50%) experience shifts in MHC composition following HS that favor an increase of fast type IIa fibers with a decrease in slow type I fibers. Further evidence for the shift in MHC composition towards a faster muscle was provided by McCarthy et al. (1997) and McCarthy et al. (1999) who found that there were significant decreases in the mRNA expression of transcripts found predominantly in slow fibers such as β-MHC, SMLC$_1$ (slow myosin light chain 1), and SMLC$_2$ (slow myosin light chain 2) in the mouse soleus following 14 days of HS. Thus, unlike the C57BL/6 mouse strain, the ICR and CBA/J strains show shifts in soleus MHC composition following non-weight bearing which are similar in direction to other models such as rat HS and human bedrest or spaceflight (Baldwin et al., 2001; Edgerton and

Roy, 1996; Widrick et al., 1999; Edgerton et al., 1995; Fitts et al., 2000). Soleus

muscles in these species are comprised predominantly of type I fibers.

In the present study, HS caused a decrease in CSA for both slow type I

fibers (ICR: 39%; CBA/J: 34%) and fast IIa fibers (ICR: 21%; CBA/J: 35%). These

changes are similar to results from other studies of HS with mice (Stelzer and

Widrick, 2002; Haida et al., 1989). It is interesting to note that the type I fiber CSA

were similar in all three strains we studied and all experienced similar atrophy (33-

39%) following HS. Type IIa fibers from the C57BL/6 and CBA/J strains were of

similar CSA and showed similar atrophy (32% and 35%, respectively). In contrast,

the type IIa fibers from the ICR strain, which were 23-25% smaller than their type

IIa counterparts from C57BL/6 and CBA/J strains, respectively, only atrophied

21% following HS. These results support Edgerton and Roy's (1996) observations

that the amount of fiber atrophy occurring following non-weight bearing is related

to fiber CSA before non-weight bearing. Regardless of fiber type, it appears that

the degree of atrophy is proportional to fiber size, with fibers of greater CSA before

non-weight bearing experiencing more atrophy following non-weight bearing.

Both strains of mouse showed significant decreases in absolute force (mN)

of single fibers expressing type I and IIa MHC with 7 days of HS. When values

were normalized for fiber CSA, both strains showed remarkable similarity in HS-

induced decreases in specific force for type I and IIa fibers. These results are

similar to our previous HS study on C57BL/6 mice and confirm that HS causes a

decrease in fiber quality in the mouse similar to reported findings with other

models of non-weight bearing such as HS rat (Gardetto et al., 1989; Thompson et al., 1998; McDonald et al., 1994) and human spaceflight and bedrest (Widrick et al., 1999).

It is interesting to note that the three mouse strains we studied all showed similar decreases in fiber force/CSA for type I and type IIa fibers despite having vastly different soleus MHC composition. This suggests that the role of the muscle, rather than the MHC content, determines the impact HS has an individual fiber's ability to produce force. Thus, our data indicate that mouse type I and type IIa fibers are equally affected by non-weight bearing with respect to a decreased ability to produce force.

Our results suggest that increases in type I fiber V_0 in the mouse soleus are not solely related to fiber atrophy since all three strains experienced significant atrophy of type I fibers following HS yet not all strains showed changes in V_0. Thus, in the fast C57BL/6 soleus, type I V_0 was unchanged by HS while in the mixed composition ICR and CBA/J solei, type I V_0 was increased.

In summary, the present study shows that the mouse is an effective model to study the effects of non-weight bearing on muscle function. Following 7 days of HS there was a significant atrophy of the soleus muscle accompanied by a shift in MHC composition that favored an increased expression of type IIa MHC and a decreased expression of type I MHC. Seven days of HS caused significant type I and IIa fiber atrophy in soleus muscles of ICR and CBA/J mice. Both strains showed decreased fiber absolute and specific force in slow and fast fibers. Maximal

shortening velocity of type I fibers of ICR and CBA/J mice increased following HS. The increase in fiber V_o in conjunction with the increased expression of type IIa MHC in both strains following HS may act as a protective mechanism to maintain whole muscle function despite decreases in fiber force. It appears that the shift in soleus MHC composition to a faster MHC isoform and the increase in fiber V_o are dependent, in part, on the MHC composition of the muscle. Muscle physiologists studying the effects of non-weight bearing on mouse muscle function should be aware that soleus muscle MHC composition varies dramatically across mouse strains and that the response of soleus muscle fibers to non-weight bearing may depend on soleus MHC composition.

Chapter 5

Conclusions

Julian E. Stelzer

Department of Exercise and Sport Science

The present project examined the protein-function relationships of mouse skeletal single muscle fibers before and following 7 days of HS. Our data show that there are differences in soleus MHC composition across mouse strains. Furthermore, the maximal shortening velocity of type I fibers differs across strains. This was demonstrated by slower than expected shortening velocities in mice that have a low proportion of soleus type I MHC. We also showed that soleus myosin heavy chain composition might be related to changes that occur in type I fiber shortening velocity following 7 days of HS. Type I fibers from mice with low soleus type I MHC composition showed no increases in shortening velocity while type I fibers from mice with a higher composition of soleus type I MHC showed an increase in V_o. These results are novel since data on protein-function relationships of skinned skeletal single fibers of mice before and following HS were not previously available.

The data in Chapter 2 elucidated the protein-function relationships in skinned fibers from the C57BL/6 mouse. This strain is the most widely studied strain in biomedical research. Specific peak Ca^{2+}-activated force was similar in all fiber types and ranged from 116 to 120 kN/m^2. The relationship between fiber type MHC expression and maximal shortening velocity (V_o) was (from slowest to fastest shortening): type I < type IIa < type IIx/IIb < type IIb. Thus, the general relationships between soleus fiber force, V_o, and protein isoform expression was found to be similar to other mammals. However, in contrast to many mammals the C57BL/6 soleus is a predominantly fast muscle, containing only 20% type I MHC.

In addition, lower than expected shortening velocities were observed for slow fibers from this muscle. The observed V_o of the IIb fibers was in good agreement with the V_o predicted for a mammal of this body mass by allometric regression equations, however, the V_o observed for the type I fibers was 25% slower than predicted. These discrepancies in predicted and observed shortening velocities may be due to the fact that animal scaling models of type I shortening velocity are mainly derived from animals that have a high composition of soleus type I MHC, such as the rat and rabbit. The use of these regression equations to predict the type I shortening velocities of fibers from mice with a low composition of soleus type I MHC may not be appropriate since there may be differences in the intrinsic velocities of these fibers. Since regression equations that predict type IIb shortening velocity are derived from fast muscles which contain a homogeneous population of fast fibers across most species, including the mouse, it is not surprising that this prediction was accurate.

The manuscript in Chapter 3 describes the first data examining the effects of HS on mouse single fiber contractile function. On the whole muscle level our data show similar atrophy of all hindlimb muscles, including the soleus, to other studies of HS in rats and mice. Extensor muscles showed more atrophy than flexor muscles. Similar rates of atrophy for rat and mouse muscle suggests that the 2-fold higher metabolic rate of the mouse has no net effect on muscle atrophy, perhaps because rates of protein synthesis and degradation are both elevated. However, in contrast to the rat model where type IIa MHC increases with HS, 7 days of HS did

not affect MHC isoform distribution at the whole muscle or single fiber levels in the C57BL/6 mouse.

Our single fiber data show that 7 days of HS significantly reduced force in C57BL/6 soleus fibers. The force deficit was due to fiber atrophy and reduced force per fiber cross sectional area. Soleus type I and IIa fibers were equally affected by HS with respect to atrophy and decreases in force, however, there was no change in V_o for either fiber type. Thus, the C57BL/6 strain of mouse responded similarly to the rat with respect to changes in fiber cross-sectional area and force following HS but not in V_o.

The fact that type I and II fibers were equally affected by HS in the present study may challenge the notion that type I fibers are preferentially targeted by non-weight bearing. Most of these data come from studies of rat and humans that do not have a large proportion of soleus type II fibers. Our data would suggest that rather than targeting specific fiber types, non-weight bearing affects the fibers recruited in specific muscles. In the case of the antigravity soleus muscle, all fiber types within that muscle are equally affected by non-weight bearing since all fiber types are likely recruited during weight bearing. Furthermore, we proposed that the difference in the response of the C57BL/6 mouse to non-weight bearing compared with the rat is related to the recruitment pattern of slow and fast fiber pools. That is, during weight bearing type I fibers are recruited almost exclusively in the rat slow soleus while the mixed C57BL/6 soleus recruits both slow and fast fibers. When weight bearing activity is removed the relative changes occurring in the mouse

reflect the decrease in recruitment of fibers expressing type I and IIa MHC while in the rat only type I fibers experience lower levels of recruitment.

Our data from Chapter 3 raised some interesting questions regarding the changes that occur in soleus muscle of the mouse in response to 7 days of HS. Since the C57BL/6 mouse did not show the same changes in type I V_o following HS as reported for the rat HS model, the question remained whether this was due to the unusual soleus MHC composition of the C57BL/6 strain or to inherent species differences between the mouse and the rat. The data in Chapter 4 address these questions.

We hindlimb suspended two strains of mice (ICR and CBA/J) that have a soleus MHC composition of about 50% type I in order to examine the possibility that the response to HS displayed by the C57BL/6 strain, was related to its predominantly fast soleus MHC composition. We found that comparable to the C57BL/6 strain, type I and II fibers of ICR and CBA/J strains showed similar atrophy and decreases in force production following 7 days of HS. Additionally, we found that there was a shift in MHC composition of the soleus muscle towards greater expression of type II MHC and less expression of type I MHC. Furthermore, we found that the maximal shortening velocities of type I fibers increased following HS for both strains. The latter two observations show responses to HS that are more characteristic of the responses reported in the rat. This would indicate that the results found in Chapter 3 are not due to species

differences between the mouse and the rat but might be related to differences in soleus MHC composition between the C57BL/6 strain and the rat.

Our results provided an interesting data driven question. While our intent was to examine the changes in contractile function soleus single muscle fibers from the mouse following 7 days of HS, we found strain-related differences of single-fiber function. For example, we found that the C57BL/6 mouse shows type I fiber maximal shortening velocity that is slower than predicted by regression equations based on animal body mass. This finding prompted us to examine the type I fiber shortening velocity of other strains with higher soleus type I MHC compositions. We found that soleus type I fiber maximal shortening velocities from mouse strains (ICR and CBA/J) containing 50% type I MHC were as predicted by regression equations based on animal body mass (Figure 5.1). These data reinforced our previous findings that muscle MHC composition, and single fiber contractile function may be related in the mouse soleus.

Results from our work have enhanced the understanding of the effects of non-weight bearing on skeletal muscle function and the mechanisms that contribute to single-fiber contractile function. Muscle MHC composition may play a role in the function of individual single fibers within the muscle. This can be an important consideration when comparing single fiber contractile function data from mice with different soleus MHC composition. These MHC composition differences can also influence the response of individual fibers to non-weight bearing. Future
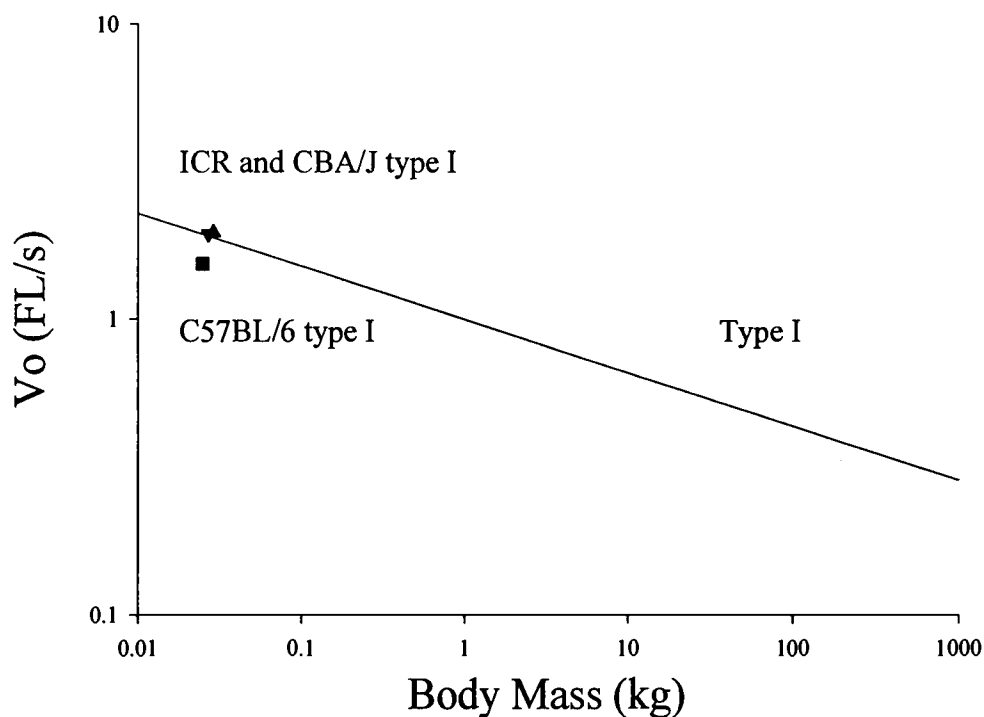
Figure 5.1 Type I shortening velocity regression equation. Log of shortening velocity versus log of animal body mass. Type I regression line taken from Rome et al. (1990) showing the effect on decreasing body mass on shortening velocity. These data depict the overestimation of average shortening velocity of type I fibers from C57BL/6 (■) mice (below the regression line) and the accurate prediction of type I fiber shortening velocity from ICR (▲) and CBA/J (▼) mice (on the regression line).

investigators should not assume that the mouse soleus muscle is a slow muscle. This is an important consideration when designing mouse transgenic or knockout models. Choosing an inappropriate strain in HS or other non-weight bearing models and making assumptions about the muscles' MHC isoform composition or response at the single fiber level can lead to erroneous conclusions.

The mechanisms responsible for the relationships between soleus muscle MHC composition and the contractile function of individual fibers are presently unclear. Future studies should investigate these mechanisms.

Bibliography

Adams, G. R., B. M. Hather and G. A. Dudley (1994). Effect of short-term unweighting on human skeletal muscle strength and size. Aviation, Space, and Environmental Medicine **65**: 1116-1121.

Agbulut, O., Z. Li, V. Mouly and G. S. Butler-Browne (1996). Analysis of skeletal and cardiac muscle from desmin knock-out and normal mice by high resolution separation of myosin heavy-chain isoforms. Biologie Cellulaire **88**: 131-135.

Andersen, J. L., T. Gruschy-Knudsen, C. Sandri, L. Larsson and S. Schiaffino (1999). Bed rest increases the amount of mismatched fibers in human skeletal muscle. Journal of Applied Physiology **86**: 455-460.

Anzil, A. P., G. Sancesario, R. Massa and G. Bernardi (1991). Myofibrillar disruption in the rabbit soleus muscle after one-week hindlimb suspension. Muscle and Nerve **14**: 358-369.

Baldwin, K. M. and F. Haddad (2001). Effects of different activity and inactivity paradigms on myosin heavy chain gene expression in striated muscle. Journal of Applied Physiology **90**: 345-357.

Bangart, J. J., J. J. Widrick and R. H. Fitts (1997). Effect of intermittent weight bearing on soleus fiber force-velocity-power and force-pCa relationships. Journal of Applied Physiology **82**: 1905-1910.

Bottinelli, R., R. Betto, S. Schiaffino and C. Reggiani (1994). Unloaded shortening velocity and myosin heavy chain and alkali light chain isoform composition in rat skeletal muscle fibres. Journal of Physiology (London) **478**: 341-349.

Bottinelli, R., M. Canepari, M. A. Pellegrino and C. Reggiani (1996). Force-velocity properties of human skeletal muscle fibres: myosin heavy chain isoform and temperature dependence. Journal of Physiology (London) **495**: 573-586.

Brooks, S. V. and J. A. Faulkner (1994). Isometric, shortening, and lengthening contractions of muscle fiber segments from adult and old mice. American Journal of Physiology Cell Physiology **267**: C507-C513.

Caiozzo, V. J., M. J. Baker, R. E. Herrick, M. Tao and K. M. Baldwin (1994). Effect of a spaceflight on skeletal muscle: mechanical properties and myosin isoform content of a slow muscle. Journal of Applied Physiology **76**: 1764-1773.

Caiozzo, V. J., F. Haddad, M. J. Baker, R. E. Herrick, N. Prietto and K. M. Baldwin (1996). Microgravity-induced transformations of myosin isoforms and contractile properties of skeletal muscle. Journal of Applied Physiology **81**: 123-132.

Caiozzo, V. J., M. J. Baker and K. M. Baldwin (1997). Modulation of myosin isoform expression by mechanical loading: role of stimulation frequency. Journal of Applied Physiology **82**: 211-218.

Caiozzo, V. J., M. J. Baker and K. M. Baldwin (1998). Novel transitions in MHC isoforms: separate and combined effects of thyroid hormone and mechanical unloading. Journal of Applied Physiology **85**: 2237-2248.

Carlson, C. J., F. W. Booth and S. E. Gordon (1999). Skeletal muscle myostatin mRNA expression is fiber-type specific and increases during hindlimb unloading. American Journal of Physiology Regulatory Integrative and Comparative Physiology **46**: R601-R606.

Corley, K., N. Kowalchuk and A. J. McComas (1984). Contrasting effects of suspension on hind limb muscles in the hamster. Experimental Neurology **85**: 30-40.

Criswell, D. S., F. W. Booth, F. DeMayo, R. J. Schwartz, S. E. Gordon and M. L. Fiorotto (1998a). Overexpression of IGF-I in skeletal muscle of transgenic mice does not prevent unloading-induced atrophy. American Journal of Physiology Endocrinology and Metabolism **38**: E373-E379.

Criswell, D. S., V. R. M. Hodgson, E. C. Hardeman and F. W. Booth (1998b). Nerve-responsive troponin I slow promoter does not respond to unloading. Journal of Applied Physiology **84**: 1083-1087.

Delp, M. D. and C. Duan (1996). Composition and size of type I, IIA, IID/X and IIB fibers and citrate synthase activity of rat muscle. Journal of Applied Physiology **80**: 261-270.

Desplanches, D., M. H. Mayet, B. Sempore and R. Flandrois (1987). Structural and functional responses to prolonged hindlimb suspension in rat muscle. Journal of Applied Physiology **63**: 558-563.

Edgerton, V. R., M.-Y. Zhou, Y. Ohira, H. Klitgaard, B. Jiang, G. Bell, B. Harris, B. Saltin, P. D. Gollnick, R. R. Roy, M. K. Day and M. Greenisen (1995). Human fiber size and enzymatic properties after 5 and 11 days of spaceflight. Journal of Applied Physiology **78**: 1733-1739.

Edgerton, V. R. and R. R. Roy (1996). Neuromuscular adaptations to actual and simulated spaceflight. Handbook of Physiology. Environmental Physiology. Bethesda, MD, American Physiological Society. II: 721-763.

Edman, K. A. P. (1979). The velocity of unloaded shortening and its relation to sarcomere length and isometric force in vertebrate muscle fibres. Journal of Physiology (London) **291**: 143-159.

Fabiato, A. (1985). Time and calcium dependence of activation and inactivation of calcium-induced release of calcium from the sarcoplasmic reticulum of a skinned canine cardiac purkinje cell. Journal of General Physiology **85**: 247-289.

Fabiato, A. (1988). Computer programs for calculating total from specified free or free from specified total ionic concentrations in aqueous solutions containing multiple metals and ligands. Methods in Enzymology, Academic Press. **157**: 378-417.

Fauteck, S. P. and S. C. Kandarian (1995). Sensitive detection of myosin heavy chain composition in skeletal muscle under different loading conditions. American Journal of Physiology Cell Physiology **268**: C419-C424.

Fejtek, M. B. and R. J. Wassersug (1999). Survey of studies on how spaceflight affects rodent skeletal muscle. Advances in Space Biology and Medicine **7**: 1-30.

Festing, M. F. W. (1994). Inbred strains of mice. Mouse Genome **92**: 373-495.

Festing, M. F. W. (1997). Inbred strains of mice: a vital resource for biomedical research. Mouse Genome **95**: 845-855.

Fitts, R. H., J. M. Metzger, D. A. Riley and B. R. Unsworth (1986). Models of disuse: a comparison of hindlimb suspension and immobilization. Journal of Applied Physiology **60**: 1947-1953.

Fitts, R.H. (1994). Cellular mechanisms of muscle fatigue. Physiological Reviews. **74**: 49-94.

Fitts, R. H., S. C. Bodine, J. G. Romatowski and J. J. Widrick (1998). Velocity, force, power, and Ca^{2+} sensitivity of fast and slow monkey skeletal muscle fibers. Journal of Applied Physiology **84**: 1776-1787.

Fitts, R. H., D. R. Riley and J. J. Widrick (2000). Microgravity and skeletal muscle. Journal of Applied Physiology **89**: 823-839.

Fitts, R. H., D. A. Riley and J. J. Widrick (2001). Functional and structural adaptations of skeletal muscle to microgravity. Journal of Experimental Biology **204**: 3201-3208.

Frontera, W. R., D. Suh, L. S. Krivickas, V. A. Hughes, R. Goldstein and R. Roubenoff (2000). Skeletal muscle fiber quality in older men and women. American Journal of Physiology Cell Physiology **279**: C611-C618.

Gardetto, P. R., J. M. Schluter and R. H. Fitts (1989). Contractile function of single muscle fibers after hindlimb suspension. Journal of Applied Physiology 66: 2739-2749.

Haida, N., W. M. Fowler, R. T. Abresch, D. B. Larson, R. B. Sharman, R. G. Talor and R. K. Entrikin (1989). Effect of hind-limb suspension on young and adult skeletal muscle. Experimental Neurology 103: 68-76.

Hämäläinen, N. and D. Pette (1993). The histochemical profiles of fast fiber types IIB, IID, and IIA in skeletal muscles of mouse, rat, and rabbit. Journal of Histochemistry and Cytochemistry 41: 733-743.

Ingalls, C. P., G. L. Warren and R. B. Armstrong (1999). Intracellular Ca^{2+} transients in mouse soleus muscle after hindlimb unloading and reloading. Journal of Applied Physiology 87: 386-390.

Ingalls, C. P., J. C. Wenke and R. B. Armstrong (2001). Time course changes in $[Ca^{2+}]_i$, force, and protein content in hindlimb-suspended mouse soleus muscles. Aviation, Space, and Environmental Medicine 72: 471-476.

Kandarian, S., O'Brien, S., Thomas, K., Schulte, L., Navarro, J. (1992). Regulation of skeletal muscle dihydropyridine receptor gene expression by biomechanical unloading. Journal of applied Physiology: Respiratory Environmental and Exercise Physiology. 72: 2510-2514.

Ku, Z., Thomason, D.B. (1994). Soleus muscle nascent polypeptide chain elongation slows protein synthesis rate during non-weight bearing activity. American Journal of Physiology: Cell Physiology. 267: C115-C126.

LaFramboise, W. A., M. J. Daood, R. D. Guthrie, P. Moretti, S. Schiaffino and M. Ontell (1990). Electrophoretic separation and immunological identification of type 2X myosin heavy chain in rat skeletal muscle. Biochimica et Biophysica Acta 1035: 109-112.

Larsson, L. and R. L. Moss (1993). Maximum velocity of shortening in relation to myosin isoform composition in single fibres from human skeletal muscles. Journal of Physiology (London) **472**: 595-614.

Liu, K. and H. K. Gershenfeld (2001). Genetic differences in tail-suspension test and its relationship to Imipramine among 11 inbred strains of mice. Biological Psychiatry **49**: 575-581.

Maher, B. A. (2002). Test tubes with tails. The Scientist **16**: 22-24.

Malakoff, D. (2000). The rise of the mouse, biomedicine's model mammal. Science **288**: 249-253.

Marechal, G. and G. Beckers-Bleukx (1993). Force-velocity relation and isomyosins in soleus muscles from two strains of mice (C57 and NMRI). Pflügers Archives. **424**: 478-487.

Matsubara, I., Y. Umazume and N. Yagi (1985). Lateral filamentary spacing in chemically skinned murine muscles during contraction. Journal of Physiology (London) **360**: 135-148.

McCarthy, J. J., A. M. Fox, G. L. Tsika, L. Gao and R. W. Tsika (1997). [t] β-MHC transgene expression in suspended and mechanically overloaded/suspended soleus muscle of transgenic mice. American Journal of Physiology Regulatory Integrative and Comparative Physiology **272**: R1552-R1561.

McCarthy, J. J., D. R. Vyas, G. L. Tsika and R. W. Tsika (1999). Segregated regulatory elements direct β-myosin heavy chain expression in response to altered muscle activity. The Journal of Biological Chemistry **274**: 14270-14279.

McDonald, K. S., C. A. Blaser and R. H. Fitts (1994). Force-velocity and power characteristics of rat soleus muscle fibers after hindlimb suspension. Journal of Applied Physiology **77**: 1609-1616.

McDonald, K. S. and R. H. Fitts (1995). Effect of hindlimb unloading on rat soleus fiber force, stiffness, and calcium sensitivity. Journal of Applied Physiology **79**: 1796-1802.

Metzger, J. M. and R. L. Moss (1987). Shortening velocity in skinned single muscle fibers. Influence of filament lattice spacing. Biophysical Journal **52**: 127-131.

Morey, E. R. (1979). Spaceflight and bone turnover: Correlation with a new rat model of weightlessness. BioScience **29**: 168-172.

Musacchia, X. J., D. R. Deavers, G. A. Meininger and T. P. Davis (1980). A model for hypokinesia: Effects on muscle atrophy in the rat. Journal of Applied Physiology **48**: 479-486.
Nishioka, Y. (1995). The origin of common laboratory mice. Genome **38**: 1-7.

Ohira, Y., B. Jiang, R. R. Roy, V. Oganov, E. Ilyina-Kakueva, J. F. Marini and V. R. Edgerton (1992). Rat soleus muscle fiber responses to 14 days of spaceflight and hindlimb suspension. Journal of Applied Physiology **73**: 51S-57S.

Pate, E., G. J. Wilson, M. Bhimani and R. Cooke (1994). Temperature dependence of the inhibitory effects of Orthovanadate on shortening velocity in fast skeletal muscle. Biophysical Journal **66**: 1554-1562.

Reiser, P. J., R. L. Moss, G. G. Giulian and M. L. Greaser (1985). Shortening velocity in single fibers from adult rabbit soleus muscles is correlated with myosin heavy chain composition. Journal of Biological Chemistry **260**: 9077-9080.

Reiser, P. J., C. E. Kasper and R. L. Moss (1987). Myosin subunits and contractile properties of single fibers from hypokinetic rat muscles. Journal of Applied Physiology **63**: 2293-2300.

Riley, D.A., Slocum, G.R., Bain, J.L.W., Sedlak, F.R., Sowa, T.E., Mellender, J.W. (1990). Rat hindlimb unloading: soleus histochemistry, ultrastructure, and electromyography. Journal of Applied Physiology. **69**: 58-66.

Riley, D. A., J. L. W. Bain, J. L. Thompson, R. H. Fitts, J. J. Widrick, S. W. Trappe, T. A. Trappe and D. L. Costill. (1998). Disproportionate loss of thin filaments in human soleus muscle after 17-day bed rest. Muscle and Nerve **21**: 1280-1289.

Riley, D. A., J. L. W. Bain, J. L. Thompson, R. H. Fitts, J. J. Widrick, S. W. Trappe, T. A. Trappe and D. L. Costill (2000). Decreased thin filament density and length in human atrophic soleus muscle after spaceflight. Journal of Applied Physiology **88**: 567-572.

Rome, L. C., A. A. Sosnicki and D. O. Goble (1990). Maximum velocity of shortening of three fibre types from horse soleus muscle: implications for scaling with body size. Journal of Physiology (London) **431**: 173-185.

Rome, L. C. (1992). Scaling of muscle fibres and locomotion. Journal of Experimental Biology **168**: 243-252.

Sartorius, C. A., B. D. Lu, L. Acakpo-Satchivi, R. P. Jacobsen, W. C. Byrnes and L. A. Leinwand (1998). Myosin heavy chains IIa and IId are functionally distinct in the mouse. Journal of Cell Biology **141**: 943-953.

Schulte, L.M., Navarro, J., Kandarian, S.C. (1993). Regulation of sarcoplasmic reticulum calcium pump gene expression by hindlimb unweighting. *American* Journal of Physiology: Cell Physiology. **264**: C1308-C1315.

Seow, C. Y. and L. E. Ford (1991). Shortening velocity and power output of skinned muscle fibers from mammals having a 25,000-fold range of body mass. Journal of General Physiology **97**: 541-560.

Shevchenko, A., M. Wilm, O. Vorm and M. Mann (1996). Mass spectrometric sequencing of proteins from silver-stained polyacrylamide gels. Analytical Chemistry **68**: 850-858.

Steffen, J. M., R. Robb, M. J. Dombrowski, X. J. Musacchia, A. D. Mandel and G. Sonnenfeld (1984). A suspension model for hypokinetic/hypodynamic and antiorthostatic responses in the mouse. Aviation, Space, and Environmental Medicine **55**: 612-616.

Steffen, J. M. and X. J. Musacchia (1986). Spaceflight effects on adult rat muscle protein, nucleic acids, and amino acids. American Journal of Physiology Regulatory Integrative and Comparative Physiology **251**: R1059-R1063.

Stelzer, J. E. and J. J. Widrick (2002). Contractile function of single fibers from slow and fast muscles of C57BL/6 mice. In review.

Stevens, L., Mounier, Y. (1992). Ca^{2+} movements in sarcoplasmic reticulum of rat soleus fibers after hindlimb suspension. Journal of Applied Physiology. **72**: 1735-1740.

Sweeney, H. L., M. J. Kushmerick, K. Mabuchi, J. Gregely and F. A. Sreter (1986). Velocity of shortening and myosin isozymes in two types of rabbit fast-twitch muscle fibers. American Journal of Physiology Cell Physiology **251**: C431-C434.

Talmadge, R. J., R. R. Roy and V. R. Edgerton (1996). Distribution of myosin heavy chain isoforms in non-weight-bearing rat soleus muscle fibers. Journal of Applied Physiology **81**: 2540-2546.

Taylor, C. R., K. Schimdt-Nielsen and J. L. Raab (1970). Scaling of energetic cost of running to body size in mammals. American Journal of Physiology **219**: 1104-1107.

Templeton, G.H., Padalino, M., Manton, J., Glasberg, M., Silver, C.J., Silver, P., deMartino, G., Leconey, T., Klug, G., Hagler, H., Sutko, J.L. (1984). Influence of suspension hypokinesia on rat soleus muscle. Journal of Applied Physiology: Respiratory Environmental and Exercise Physiology. **56**: 278-286.

Templeton, G.H., Sweeney, L., Timson, B.F., Padalino, M., Dudenhoefter, G.A. (1988). Changes in fiber composition of soleus muscle during rat hindlimb suspension. Journal of applied Physiology: Respiratory Environmental and Exercise Physiology. **65**: 1191-1195.

Tikunov, B. A., H. L. Sweeney and L. C. Rome (2001). Quantitative electrophoretic analysis of myosin heavy chains in single muscle fibers. Journal of Applied Physiology **90**: 1927-1935.

Thomason, D.B., Baldwin, K.M., Herrick, R.E. (1986). Myosin isozyme distribution in rodent hindlimb skeletal muscle. Journal of Applied Physiology: Respiratory Environmental and Exercise Physiology. **60**: 1923-1931.

Thomason, D.B., Biggs, R.B., Booth, F.W. (1989). Protein metabolism and β-myosin heavy-chain mRNA in unweighted soleus muscle. American Journal of Physiology: Regulatory Integrative Comparative Physiology. **257**: R300-R305.

Thomason, D.B, Booth, F.W. (1990). Atrophy of the soleus muscle by hindlimb unweighting. Journal of Applied Physiology: Respiratory Environmental and exercise Physiology. **68**: 1-12.

Thompson, L. V., S. A. Johnson and J. A. Shoeman (1998). Single soleus muscle fiber function after hindlimb unweighting in adult and aged rats. Journal of Applied Physiology **84**: 1937-1942.

Tsika, R. W. (1994). Transgenic animal models. Exercise and Sport Sciences Reviews. J. O. Holloszy. Baltimore, Williams and Wilkins. **22:** 361-388.

Walmsley, B., Hodgson, J.A., and Burke, R.E. Forces produced by medial gastrocnemius and soleus muscles during locomotion in freely moving cats (1978). Journal of Neurophysiology. **41**: 1203-1215.

Warren, G. L., D. A. Hayes, D. A. Lowe, J. H. Williams and R. B. Armstrong (1994). Eccentric contraction-induced injury in normal and hindlimb-suspended mouse soleus and EDL muscles. Journal of Applied Physiology **77**: 1421-1430.

Wernig, A., A. Irintchev and P. Weisshaupt (1990). Muscle injury, cross-sectional area and fibre type distribution in mouse soleus after intermittent wheel-running. Journal of Physiology (London) **428**: 639-652.

Widrick, J. J., J. J. Bangart, M. Karhanek and R. H. Fitts (1996). Soleus fiber force and maximal shortening velocity after non-weight bearing with intermittent activity. Journal of Applied Physiology **80**: 981-987.

Widrick, J. J., J. G. Romatowski, M. Karhanek and R. H. Fitts (1997). Contractile properties of rat, rhesus monkey, and human type I fibers. American Journal of Physiology Regulatory Integrative and Comparative Physiology **272**: R34-R42.

Widrick, J. J., S. K. Knuth, K. M. Norenberg, J. G. Romatowski, J. L. W. Bain, D. A. Riley, M. Karhanek, S. W. Trappe, T. A. Trappe, D. L. Costill and R. H. Fitts (1999). Effect of a 17 day spaceflight on contractile properties of human soleus fibers. Journal of Physiology (London) **516**: 915-930.

Widrick, J. J. (2002). Effect of P_i on unloaded shortening velocity of slow and fast mammalian muscle fibers. American Journal of Physiology Cell Physiology **282**: C647-C653.

Widrick, J. J., J. E. Stelzer, T. C. Shoepe and D. P. Garner (in press). Functional properties of human muscle fibers after short-term resistance exercise training. American Journal of Physiology Regulatory Integrative and Comparative Physiology.

Zardini, D. M. and D. J. Parry (1994). Identification, distribution, and myosin subunit composition of type IIX fibers in mouse muscles. Muscle and Nerve **17**: 1308-1316.

Zhou, M.-Y., H. Klitgaard, B. Saltin, R. R. Roy, V. R. Edgerton and P. D. Gollnick (1995). Myosin heavy chain isoforms of human muscle after short-term spaceflight. Journal of Applied Physiology **78**: 1740-1744.